Moisture Transport and Changes in Mechanical Properties in Oriented Strand Board: Experimental and Modeling

by

Rodrigo Javier Araya Olguín

A thesis submitted in partial fulfillment of the requirements for the degree of

Master of Science

Department of Renewable Resources

University of Alberta

Abstract

The demand by the building industry for engineered wood composites is continuously increasing due to its importance as a structural building material. Even though the forest products sector is constantly working to find solutions to improve the design of material properties, research to predict the performance of wood-based composites in service (e.g., subject to moisture) for different manufacturing variables are limited. The objective of this thesis was to investigate and predict the moisture content and transport in unidirectional oriented strand board (OSB) based on various material and manufacturing parameters including strand grain direction, wax content, and panel density. In addition, the effect of moisture content on changes to mechanical properties including modulus of elasticity (MOE) and modulus of rupture (MOR) were also studied. A three-dimensional finite element model (FEM) was developed to predict the moisture distribution in unidirectional OSB panels, and was used to determine the effective diffusivity coefficients of various panel parameters based on a series of moisture absorption experiments. The FEM was based on Fick's second law which was found to provide an accurate fit with the experimental data during the first stages of moisture ingress.

The results showed that the moisture absorption and diffusivity coefficients of OSB panels were greater with decreasing panel densities, and were also greater for specimens without wax and in strand directions perpendicular to the grain. Specifically, the results show that a higher strand-strand contact or compact structure of the board reduced the void spaces, thus reducing the migration of water molecules to the board. Wax is another manufacturing variable which affects the moisture absorption and diffusivity coefficient. In the experiments, waxed and un-waxed OSB specimens were tested, and the results indicate that strands treated with the water-repellent additive reduced the water absorption rate in OSB but did not prevent overall moisture saturation (i.e. wax

simply delayed moisture transport). The grain direction of the strands was another factor affecting the diffusivity coefficient and water transport behaviour in composite boards. The findings show that water uptake parallel to the strand grain direction was greater than in the perpendicular to grain direction due to the natural structure of the aligned wood cells (lumen).

In addition, the findings show that board density, moisture content and grain direction have a significant effect on bending properties. The MOE and MOR of panels both decreased as panel moisture content increased. At lower average moisture contents, the panel density had a much more significant effect on bending properties relative to higher moisture contents (>25%) where changes in board density did not significantly affect bending properties. Overall, wax content did not show any significant effects on MOE and MOR at a given average moisture content. The resulting MOE and MOR datasets for unidirectional OSB panels were also fit to a polynomial mathematical model with first order coefficient for density and second-order coefficients for moisture content.

The results obtained from this research provides valuable information on further understanding and modeling of moisture absorption/distribution in OSB panels exposed to water. Tests performed on unidirectional panels also provide a unique set of basic property data at the ply level which can be used in subsequent studies to create more complex models of real OSB systems (e.g., commercial panels). These predictive tools could then be used to possibly improve OSB performance and durability in existing and new applications.

Preface

The research presented in this thesis is an original work of Rodrigo Araya Olguín under the supervision of Dr. John Wolodko. There are 5 chapters in this thesis. Chapter 1 contains introduction and the objectives of this research. Chapter 2 presents literature review related to this thesis. Chapter 3 is a self-contained manuscript focused on the following: (a) effect of wax content, grain directions, and board density on the water diffusivity and total weight gain of unidirectional OSB and (b) simulation of the moisture transport in OSB panels as a function of local density and wax content using a finite element model (FEM) based on Fick's law. Chapter 4 is also a self-contained manuscript which presents an exhaustive study about the effect of moisture content on the mechanical properties (including thickness swell, MOE and MOR) of unidirectional OSB panels as a function of wax content, grain directions, and board density. Chapters 3 and 4 will both be submitted to relevant journals for publication. Finally, in Chapter 5, most relevant results and future prospects of the research are discussed.

Acknowledgements

I would like to thank my supervisor Dr. John Wolodko for all of his guidance and support throughout all my research. In addition, I would also like to thank to Dr. Siguo Chen from InnoTech Alberta who provided significant advice and feedback to my research. Last of all, I would like to thank my wife, Karina, and my son, Matías, for their consistent patience, love, and encouragement to finish this thesis.

Table of contents

List of Tables

List of Figures

Chapter 1: Introduction and objectives

Oriented Strand Board (OSB) is an important engineering wood composite manufactured from a mixture of thin wood strands with waterproof resins, which are bound together under heat and pressure. The OSB manufacturing process includes many steps: log debarking; stranding; strand drying; blending; hot pressing; mat consolidation; finishing line, and storage [1]. OSB is commonly used as structural elements in building construction including walls, floors, roof sheathing, insulate sandwich panels and I-shaped beams, or as non-structural elements in applications such as packaging boxes, furniture, and pallets [2]. In the last few decades, the demand for OSB has increased significantly and has become an important segment of the forest products industry. According to the Food and Agriculture Organization of the United Nations (FAO) [3], Canada is the second largest producer of OSB (Fig. 1.1A). Moreover, OSB production in Canada increased from 4 Mm^3 in 2009 to 6.8 Mm^3 in 2019 (Fig. 1.1B).

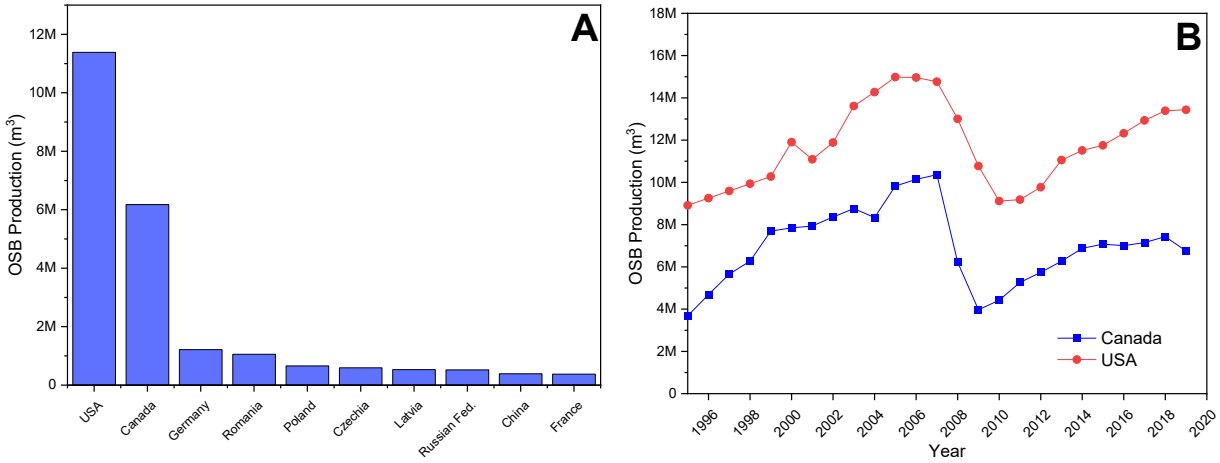

Figure 1.1 (A) Top 10 countries of average OSB production from 2009 to 2019, (B) OSB production in Canada and USA *versus* years [3]

The growing demand of OSB can be attributed to its advantages compared with other forest products such as solid wood and plywood. OSB is replacing plywood in structural panels due to its lower cost and comparable mechanical properties such as strength and stiffness under bending, shear, tension, and compression [4, 5]. One of the most significant advantages of OSB compared to plywood is its higher recovery factor [6], and that it can be produced with lower quality/smaller diameter logs or cheaper woods [7]. While OSB is seeing increased usage in building construction, one of the most important disadvantages is its intolerance to adverse environmental conditions such as moisture. Due to the hygroscopic nature of the wood strands and the internal structure in OSB, moisture absorption and transport can occur in OSB when it is exposed to humidity or liquid water. This can result in undesirable physical changes in the panel including thickness swell (TS), and linear expansion (LE), loss of strength and stiffness [8], and cause mold proliferation [9]. These drawbacks, unfortunately, limit its use especially when the panels are directly exposed to adverse environmental conditions. As a result, mitigation of OSB exposure to moisture is critical both in terms of storage (e.g., proper plastic wrapping of OSB sheets) and application (e.g., using siding or stucco to protect OSB wall sheathing).

The OSB industry is continuously working to optimize the production process parameters (e.g., wood species, strand moisture content, type and amount of resin, fines content, pressing temperature and pressing time) to improve the durability, dimensional stability and building performance of OSB, and to reduce its manufacturing cost. For example, numerous studies have shown that the physical and mechanical properties of OSB can be enhanced by many factors such as strand geometry and orientation; surface/core ratios [10–13]; amount of fines [14–16]; wood species [17, 18]; wax type and resin/wax ratio [19–21]. One of the most important properties in OSB is the density of the panel (both average and local) which directly affects the mechanical and

other characteristics of the manufactured panel [17, 21–23]. In general, the non-homogeneous distribution of density within an OSB panel can also have a negative effect on a number of mechanical properties in OSB including modulus of elasticity (MOE), modulus of rupture (MOR), internal bond (IB), and can promote thickness swell (TS), water absorption, and linear expansion (LE) [21]. While panel density is known to play a significant role in OSB performance, there is still limited data on how density affects moisture absorption behaviour.

In terms of usage, the OSB industry continues to improve the quality and durability of their panels, and now offers panels for specific applications (e.g., wall sheathing versus flooring). For this reason, a model capable of predicting the effects of different parameters on the performance of panels would be a helpful tool. The finite element method (FEM) is a common engineering modeling approach employed to analyze physical phenomena in the fields of structural/solid mechanics, fluid mechanics, heat transfer, mass transfer and others in order to reduce cost and improve process design. Mackerle [24] published a review with more than 200 studies using FEM in wood and wood composites. However, there are still limited studies using FEM that focus on OSB and the effect of water absorption. Modeling of the performance of OSB is also a challenge for researchers due to its non-homogenous composition, and the variability in the experimental data under the same operational conditions. A model capable of predicting water transport and moisture effects on the physical stability and mechanical strength of OSB might be a useful tool to reduce cost and improve quality standards.

The main objective of this thesis is to contribute to a better understanding the effect of the transient moisture movement on the mechanical properties of OSB panels in terms of varying panel density, wax content, grain direction, and moisture content. To achieve the goal, the following specific objectives were addressed:

1. To experimentally study the weight gain and water diffusivity behavior of OSB panels as a function of grain direction, wax content, and board density, and to simulate the planar moisture transport in OSB panels as a function of local density and wax content using the finite element method based on Fick's law (Chapter 3),

2. To develop a mathematical model and investigate the influence of moisture content on the mechanical properties (including MOE and MOR) and dimensional stability (thickness swell) of unidirectional OSB panels as a function of wax content, grain direction, and board density (Chapter 4).

Chapter 2: Literature review

2.1 Introduction to Oriented Strand Board (OSB)

Oriented Strand Board (OSB) is a wood composite which is composed of approximately 94-97% wood strands, and 3-6% of resin and 1-1.5% of wax [6, 25, 26]. Steps involved in OSB manufacturing start with debarking logs and then cutting them into thin and elongated wood elements called strands using a strander cutting machine. OSB strands can be characterized by their thickness, width, length, and slenderness ratio (the ratio of length to thickness). The typical dimensions of OSB strands are 75 - 150 mm long, 15 - 25 mm wide, and 0.5 - 0.7 mm thick [27, 28]. In the next step, the strands are then conditioned and blended with waterproof thermosetting resins and other additives (e.g., wax or biocides). Posteriorly, the oriented layers of strands are arranged within a loose mat, where usually the face layers are oriented parallel to its length while the core layer is cross-oriented. This oriented mat is then consolidated in a press using heat and pressure with temperatures over 200°C and pressures in the range of 4 to 6 MPa. Once pressed, a consolidated panel with rough edges is created which is then trimmed to meet required size specification. The final product is a panel with a complex geometric layout which offers low variability on mechanical properties under the same manufacturing conditions [26, 29, 30].

2.2 Impact of strand, resin, and wax on OSB properties

Different studies have reported the factors that affect the physical and mechanical properties of OSB. For example, strand geometry, slenderness ratio and strand angle [29, 31–33], orientation and surface/core ratios [34], amount of fines, wood species, type and amount of resin, resin/wax ratio [19, 23, 35], average and profile of density [36], and moisture content [37].

Strand source and geometry both play a role in the performance of OSB, and can be produced from a variety of tree species (such as Aspen, Southern Pine, Spruce, Birch, Yellow-Poplar, Sweetgum, Sassafrass, and Beech) using a single wood species in the entire panel or a mixture of wood species [1]. Many studies have investigated the effect of strand geometry, strand orientation, and strand moisture content on mechanical properties of OSB such as modulus of rupture (MOR), modulus of elasticity (MOE), and internal bond (IB). Wang and Lang [32, 33] reported that MOE, MOR, and IB of OSB increased with increasing strand length. Based on their experiments, the authors established the optimum slenderness ratio between strand length and strand thickness to optimize the mechanical properties, and determined an empirical relationship between the mechanical properties and strand angles. Similarly, Barnes [10, 38, 39] developed an empirical model that predicted tensile strength, MOR, and MOE. The author concluded that increasing strands length improved the OSB bending properties. Moreover, the results indicated the importance of the effect of strand-to-strand contact on the capacity to transfer stress within the panel.

A similar finding was reported by Meyers [34] who pointed out that mechanical properties of OSB are strongly influenced by strand orientation and geometry. Long strands lengths tended to increase the overlap-length and improved the capacity to transfer stress which was found to

increase the tensile strength. Similar results were also observed by Nishimura et al [40] who reported that strands with a higher aspect ratio (length divided by the width) produced panels with better mechanical properties, specifically, MOE and MOR under bending. In addition to strand geometry, mat forming conditions and its effect on OSB properties has also been investigated. Chen et al [11] reported the effect of the mat structure on the MOE of OSB. The study showed the importance strand alignment on the surface layer, specifically, that an increase face to core ratio enhanced the effective MOE parallel to the grain.

In general, there are four main types of resins used in OSB [41]: phenol formaldehyde (PF), urea formaldehyde (UF), melamine formaldehyde (MF) and isocyanate compounds. Previous studies have reported a positive effect of resin content on mechanical and physical (or dimensional) properties of boards, mainly attributed to the increase in cell wall bulking and intra-cell bonding. For instance, Taylor et al [42] indicated that thickness swell and water absorption in OSB improved as resin levels increased. In addition, Brochmann et al [19] concluded that using more hydrophobic resins in the core layer of OSB increased the dimensional stability and water resistance of boards. Zhang et al [43] pointed out the negative effect of employing low resin and low wax content on the water uptake behavior of strands, specifically that lower resin and wax content increased the water uptake kinetics and increased the total amount of water absorbed by the OSB panel. Additionally, their findings indicated that the rate of water absorption was faster along the parallel-to-grain direction *versus* the perpendicular-to-grain direction. Moreover, strands with higher density decreased the total water uptake amount.

Neimsuwan et al [44] reported that water vapour sorption on OSB was more sensitive to the wax content than resin content. Furthermore, the authors reported that higher wax content reduced the total water uptake amount and decreased the water uptake rate. Additionally, the

diffusion coefficient of wax-free strands was significantly higher than waxed strands. Winistorfer et al [35], observed an inverse relationship between wax content and water absorption. Furthermore, a higher wax content was found to reduce the board dimensional stability due to negative effect on the adhesive curing.

2.3 Impact of vertical density profile and horizontal density distribution on OSB properties

Engineered wood panels are characterized as having a non-homogeneous density distribution. Numerous investigations have reported that the quality and stability of OSB are influenced by the average density, the density profile through the panel thickness (also known as vertical density profile or VDP), and the planar density distribution in the parallel and perpendicular board plane (also known as horizontal density distribution or HDD). VDP describes the density variation through the panel thickness, and is typically influenced by the combination of effects such as, moisture content of the strand before pressing, pressing closure rate, heat transfer during the hot-pressing process, and resin content [23, 36]. HDD describes the variability of density throughout the plane of the panel, and is mainly influenced by the mat-forming process and geometric properties such as strand size, orientation, and distribution [45, 46].

According to the literature, VDP has been reported as one of the main parameters affecting OSB properties such as MOR, MOE, and IB. Xu and Suchsland [47] and Xu [48] developed theoretical models to predict the panel MOE by assuming wood composites with uniform and non-uniform VDP. Xu & Suchsland [47] used a model based on the assumption of elasticity and all particles bonded together. This study concluded that the MOE increased linearly with the increase of either board density or compaction ratio, and that the panel MOE was not influenced by particle size. In addition, the authors found that the MOE decreased when the out-of-plane orientation of

particles increased, and that the in-plane orientation improved the panel MOE in the orientation direction but reduced MOE across the orientation direction. Xu (1999) [48] used laminate theory to simulate the effect of non-uniform VDP on the panel MOE. The model predictions indicated that the layers near the surface have an important impact on the MOE, and the panel MOE increased linearly with an increased in peak density. Jin et al [49] tested OSB panels with both uniform and conventional vertical density profiles. The authors used laminated beam theory and the regression equation from the uniform boards to predict the bending MOE in the panels. Their results indicated that the predicted MOE of non-uniform and uniform strand boards were linearly correlated to the board density (difference < 10%), and that the bending MOE of non-uniform strand boards improved only at higher density levels. Their study also found that a peak density location toward the surface is essential to maximize the MOE of the panel, and that IB, MOR, MOE, and water absorption were positively correlated with the average board density. Similarly, Linville [21] pointed out that IB is also related to VDP, specifically that IB failure might be expected in lower density layers. As a result, uniform density profiles might provide the maximum benefit to improve IB. Bozo [50] conducted a statistical analysis to find a relationship between mechanical properties of OSB with VDP and HDD. His study indicated an evident relationship between density and OSB properties, and reported that employing local density variation in mechanical analysis for concentrated static load (CSL) behaviour is more suitable than using an average global density. Chen et al [51] conducted a study to investigate the effects of panel density on parallel MOR, parallel MOE, IB, and parallel and perpendicular rolling shear strength on OSB. The authors manufactured panels with a density range between 449 to 705 kg/m^3. The findings indicated that panel density positively affected the physical and mechanical properties of the OSB panels. Furthermore, the results indicated that the effects of panel density on parallel MOR and

MOE, IB, and rolling shear strength were nonlinear and might be described with convex quadratic curves. In terms of water-related properties the studied found that thickness swell and water absorption behaviour after a 24 hours soak period linearly decreased with increasing panel density.

2.4 Impact of water absorption on OSB properties

Moisture is an important factor that negatively affects the performance and service life of OSB panels. The main problems associated with moisture absorption in OSB panels include mold proliferation, shrinkage and buckling, strength reduction, and increased in thickness swell (TS) which promotes internal stresses causing losses of strength and stiffness [37]. According to van Houts et al [52], the inter-strand void spaces generated as a result of strands overlap and areas with lower density on the OSB panel are the main route for moisture movement and absorption, and consequently, changes to the OSB panel.

Several studies have investigated the effect of moisture absorption on wood-based composites. Wu and Suchsland [53] related the moisture content (MC) to TS, linear expansion (LE), and bending properties of OSB panels. The main findings were that an average change in thickness swell close to 20% was associated with MC increases from 4 to 24%. Also, MOR and MOE (perpendicular and parallel) decreased linearly with changes to MC. As MC was increased from 4% to 24%, there was an average loss of 72% and 58% for MOE and MOR, respectively, in the parallel direction, and an average loss of 83% and 67% for MOE and MOR, respectively, in the perpendicular direction.

Xu and Winistorfer [54], studied the influence of water exposure on the constituent layer of medium density fiberboard and OSB panels. The layer density showed a positive linear correlation with internal bond (IB) and TS. The authors also concluded that the high-density

surface layers are the most important areas that promoted dimensional changes on OSB panels. Later, Xu et al [55] determined the water absorption profile of OSB panels immersed in water employing a special radiation absorption technique. The study concluded that the low-density surface regions contributed more to the overall water absorption in the OSB panel as compared to the high density regions.

In addition to full immersion of specimens in water, the effect of relative humidity on OSB properties and performance has also been studied. Moya et al [56] examined the effect of cyclic relative humidity (RH) exposure on average MC and TS in OSB, and developed an empirical model to study its effect. Their research concluded that the greatest change in MC and TS was reached during the first week of the sorption phase, and a non-recoverable TS was observed after each cycle. The authors also investigated the effect of sealing the edges of the OSB panels. This proposed mitigation procedure reduced moisture gain and swelling during the sorption phase, and decreased the thickness shrinking and moisture loss at desorption. However, it was found that swelling rate was unaffected.

Lee and Wu [57] studied the bending properties and in-plane swelling of three-layer OSB, and investigated the influence of strand alignment, strand weight ratio, VDP, resin content, and MC levels. The findings reported that flake alignment and flake weight ratio were the two principal parameters that affected the lineal expansion, MOR, and MOE. They also proposed a mathematical model based on lamination theory to predict the effective modulus, linear expansion, and internal swelling stresses. The model predicted that the relationship between linear expansion and MC change was curvilinear with larger swelling rates at lower MC values. Wu et al. [58, 59] studied the long-term behavior of OSB under cyclic humidity exposure conditions. The authors were able to predict the equilibrium moisture content through the thickness of the panel as a function of the

relative humidity conditions. They reported that TS for the first cycle increased with an increase in MC level and panel density, and decreased with an increase in resin content.

Wu and Piao [8] tested four commercial OSB panels to investigate the swelling behavior and its relationship to IB strength losses under direct contact with water and high humidity exposure. The findings indicated that the total TS and non-recoverable TS reached 31.1% and 19.8%, respectively, and a IB strength loss of 62.9% as the MC was increased to 25%. It should be noted that these results did not show any significant differences in non-recoverable TS and IB strength loss for MC changes up to 7% and 8%. Moreover, an IB strength loss of about 0.3 kPa for every % of non-recoverable TS was also reported.

In addition to cyclic humidity tests, there have also been a number of studies that have investigated the entire life cycle of a wood panel in service simulating both high and low humidity levels and/or aging. Mirski and Derkowski [60] studied the bending strength of commercial OSB panels subjected to a boiling test (for 2 hours). All panels tested were manufactured using an isocyanate adhesive in the core layers and melamine urea phenol formaldehyde resin in the face layers. The results showed a decrease in strength of 50% on average. These results were even higher than the requirement for boards exposed to the accelerated ageing test. Posteriorly, Radoslaw et al [61] determined the properties of commercial OSB panels after several cycles of accelerated aging tests, and compared the results with the properties of boards exposed to outdoor conditions. The study showed that the board damage increased with each consecutive cycle. After the first cycle, the relative change in MOE, MOR, and IB were about 65, 60 and 85%, respectively.

In terms of long-term mechanical properties, Pu et al [62] studied the flexural creep behavior of sweetgum OSB made with two levels of resin content (phenol-formaldehyde), and investigated the influence of load level and relative humidity. The findings reported that higher

relativity humidity (95%) showed a great influence on the creep resistance and relative creep. At constant low relativity humidity (65%), improvement of relative creep was observed when the resin content was increased under constant 95% or cyclic 65% to 95% relativity humidity. Lars et al. [63] studied the effect of surface coating (water-repellent siding stain) on the rate of creep in commercial OSB with cyclic humidity environment. This study found that the surface coating reduced flexure creep behavior under cycling humidity on the compression side but did not appear to have a significant effect on the tension side of the specimens. Vun et al [64] monitored the creep-rupture in large specimens of commercial OSB for four equilibrium moisture contents (EMC) employing a acoustic emission technique. The study concluded that the specimens exposed to high EMC conditioning had a high thickness swell which adversely affected panel resistance to creep. The author proposed an empirical relation for the impact of creep-rupture at the various test conditions based on the percentage change of either creep factor (ratio of the net creep deflection to the instantaneous elastic deflection) or creep modulus based on the instantaneous elastic deformation.

Finally, the effect of moisture content on the thermophysical properties (such as thermal conductivity and specific heat capacity) of wood materials have also been studied. Rice and Redfern [65] found that the heat capacity of wood materials changed by about 18% as a moisture content changed from 6 to 15%. Also, Vololonirina et al [66] reported that the thermal conductivity of wood materials showed a linear increases with higher MC level. All these studies demonstrated that MC has a marked influence on the mechanical and physical properties of OSB. Therefore, moisture uptake has an important role in panel behaviour.

2.5 Mathematical models used to predict the behaviour of OSB under different operational conditions

The finite element method (FEM) is a well-developed tool used for analyzing a wide range of physical phenomena from deformation and stress in the field of solid mechanics, heat and fluid flow in the field of heat transfer and fluid mechanics, as well as for the solution of magnetic problems, amongst others. The concept behind FEM involves breaking down the partial differential equations that described the laws of physics for space-time-dependent problem into a simple and manageable approximation of the mathematical problem. FEM divides the complex geometries into segments called finite elements which are interconnected at specific points called nodes. This process results in a set of simultaneous algebraic equations which approximate the original continuous differential fields of the real solution. Current modeling tools also allow for the integration and coupling of various multi-physics approaches within one model (e.g., heat transfer with solid mechanics).

In terms of possible applications of FEM, moisture transport in a variety of materials, including wood and wood-based composites, has been studied in the literature. Liping and Deku [67] described the moisture transfer process in particleboard using FEM based on Fick's second law. This 2D model of moisture transfer assumed isotropic diffusion in the plane of the board. The model was solved under the Galerkin Method of Weighted Residual using the boundary condition of the gradient. The diffusion coefficients and surface emission coefficient were obtained experimentally from the variations of weight over time using the equation proposed by Siau [68]. This study showed a good agreement between simulated and experimental results with the error within 10%. Tackie et al 2008a [69] developed a finite element model that predicted thickness-swell of OSB based on the 3-D density distribution. The model accounted for horizontal and

vertical density variations of the panel, and predicted the moisture changes using the transient unsteady-state moisture transfer equation developed by Cloutier [70] and coupled moisture-density-stress-strain relations. The model predicted the thickness-swell of the panels after soak tests with the results showing an error of less than 10%. Later, Tackie et al [71] developed a finite element model based on the 3-D density variation of the OSB to predict the thickness-swell, density changes, resin content, and internal stresses during a 24 hour soak test. The model was validated by a comparison of experimental results, and was able to quantify the effects of resin content changes on thickness swell. In addition, the model also allowed for the examination of internal stresses and bond failures in an OSB specimen.

In addition to the finite element approach, the mechanical properties in wood composites have also been studied using simple mathematical models (e.g., empirical). For instance, Chen et al [51] used linear and quadratic regressions to investigate relationship between major properties (MOR, MOE, IB, water absorption, and TS after 24-h soaking and rolling shear strength) of OSB as a function of panel density (449 to 705 kg/m^3). The authors found that TS and water absorption linearly decreased with increasing the board density. Moreover, they reported that OSB panels with higher densities absorbed water more slowly, reducing the rate of TS. Barbuta et al [22] determined the regression equations to predict the unidirectional strand board mechanical properties as a function of density (550, 700, and 850 kg/m^3) and moisture content (20 and 50% RH at 20°C). The results indicated that the mechanical properties of the panels improved as panel density increased, however, relative humidity did not have a significant effect on mechanical properties. Chen et al [72] modeled the effect of panel properties on the CSL tests of OSB. The authors employed a simple linear regression method and a stepwise multi-linear regression technique to determine the relationship between CSL deflection with board thickness, local

density, MOE, MOR, and interlaminar shear strength. The simple linear regression method showed CSL performance was correlated with the local and average thicknesses of the OSB, local and average board densities, MOE (major direction), MOR (major direction), and shear strength (major direction). The stepwise multi-linear regression analysis showed an important reduction in CSL deflection at higher MOE (major direction), under applied loads of 890 N. Moreover, the ultimate load capacity on CSL significantly increased at higher shear strength in the major direction.

Chapter 3: Effect of local density and wax content on 2D moisture diffusion in oriented strand board

3.1 Introduction

Oriented Strand Board (OSB) is an important engineering wood composite. The main applications of OSB are as structural elements in building construction such as wall and roof sheathing, sub-floor, insulated sandwich panels, and as webs in I-shaped beams, as well as in as non-structural elements in applications such as packaging boxes, furniture, and pallets [2]. There are numerous published studies highlighting both physical and mechanical properties (quality and stability) of OSB and the influenced of panel density and wax content [11, 17, 51, 53, 54, 73, 74]. In addition, the absorption and/or desorption of moisture into wood-based composites can negatively affect their properties and reduce their service life, ultimately, limiting its use. As a result, the OSB industry has worked to find solutions to mitigate the negative effect of moisture uptake. That being said, moisture absorption in wood continues to be one of the most important physical parameters that affects the service life and dimensional stability of wood-based panels.

Moisture absorption in OSB can cause both dimensional changes and losses of strength and stiffness [37]. Previous studies have reported that the main routes for moisture movement and absorption in the panel are void spaces between the strands generated as a result of strand overlap and areas with a low density [52, 75]. Furthermore, previous researchers have concluded that the moisture absorption of OSB is affected by wax content where higher wax content reduces the total water uptake amount and decreases the water uptake rate [44, 76].

In terms of modeling this process, Fick's laws have been commonly applied to describe the diffusion of moisture in wood and wood-based composites [67, 75, 77–80]. Liping and Deku

[67] were able to describe the moisture transfer process in particleboard with a good agreement (10% error) between simulated and experimental results using a 2D Finite Element Method (FEM) based on Fick's second law. Although acceptable results were obtained, the diffusion in panel plane was assumed to be isotropic. Wu and Suchsland [78] predicted the moisture content and gradient for multi-ply wood composite panels using a model based on Fick's second law. In this case, the model did not consider the diffusion through the edges of the samples. Shi [80] developed a diffusion model based on Fick's second law to describe the moisture absorption process in wood fiber-based composites. The findings indicated a systematic prediction error for the moisture absorption process, especially at the initial stage of the moisture uptake process.

The steady and unsteady state diffusion coefficients of moisture movement in wood and wood-based composites have been determined in a number of studies. Cai and Shang [67] described the moisture transfer process in particleboard using FEM based on Fick's second law. The model was solved under the Galerkin Method of Weighted Residual using the boundary condition of the gradient. The diffusion coefficients and surface emission coefficients were obtained experimentally, and calculated the equation proposed by Siau [68]. This study showed a good agreement between simulated and experimental results (error within 10%). Cai and Wang [81] studied the steady state and unsteady state diffusion coefficients in particleboards using methods proposed by Siau [68]. The results indicated that the steady state and unsteady state diffusion coefficients parallel to panel surface were much larger than those perpendicular to panel surface. Specifically, the diffusion coefficients parallel to the panel surface were found to be 3-5 (unsteady state) and 10-20 (steady-state) times larger than those observed in the perpendicular direction. However, according to Thomen [82], the equation proposed by Siau [68] (and used by Cai and Shang [67] and Cai and Wang [81]) to determined the diffusion coefficients is only

appropriate if applied within an infinitesimally small moisture content range, since the relationship between moisture content and relative humidity is not linear. Therefore, the method proposed by Siau [68] might be not appropriate to determine the diffusion coefficient in wood or wood-based composites. Finally, moisture diffusion in other anisotropic materials (e.g., fiber reinforced polymeric composites) have also been extensively studied. For example, Pierron et al [83] proposed a novel method to identify 3D moisture diffusion parameters of glass-epoxy composites from gravimetric experimental curves based on an optimization algorithm, and has been widely used in fiber thermoset composites [84–87].

Despite these valuable contributions, comprehensive studies examining the effect of density, wax content, and grain orientation in OSB are still limited. In addition, there is a lack of understanding to develop a mathematical model capable to predict the moisture transport in OSB Therefore, the experimental characterization of basic OSB geometries and properties for each layer is a critical first step. This requires the manufacturing and testing of unidirectional OSB panels that are homogeneous through the thickness (i.e. a uniform vertical density profile).

The main objectives of this study are to investigate and model the effect of panel density, grain direction, and wax content on the moisture absorption behavior of three-layer OSB panels with strands oriented in only one direction for all layers (unidirectional) and with uniform vertical density profiles. The objective of this unidirectional and homogeneous panels is to illustrate each of the multi layers of a OSB. This comprehensive experimental approach will provide us a unique set of data at the ply level which will be used as an input for a 3D finite element model (FEM) based on Fick's law to predict the moisture movement of commercial OSB system. The model will account for local density variations in the panel, strand orientation and wax content, and will be used to generate planar moisture content profiles/maps at different average moisture content levels.

These results will then be qualitatively validated using moisture profiles generated by full-field X-ray tomography.

3.2 Materials and methods

3.2.1 Materials and manufacturing process

Three-layer unidirectional oriented strand boards were manufactured at InnoTech Alberta's wood composite panel pilot plant (Edmonton, Canada). The OSB panels were manufactured with commercial Aspen strands obtained from a local OSB mill, and had average dimensions of 108 mm in length and 0.86 mm thick. The fines were removed (sieved) using a 4.76 mm deck screen to minimize the influence of non-uniformity of fines distribution in the furnish. The face and core strands were blended in a rotary drum blender (Coil Manufacturing Ltd., Surrey, Canada) with 3.5% w/w (based on oven dry weight) liquid phenol-formaldehyde resin (Hexiom Primax^{TM} AB17A6H, 48% of solids) and either 0 or 2% w/w (based on oven dry weight) E-wax Slack (Hexion EW58S, 58% of solids). The resin content chosen was similar to values used in commercial panels, and the two wax levels chosen (0% and 2%) were chosen with the aim to generated clear differences in moisture absorption responses. The mats were then formed by hand using a forming box (865 mm x 865 mm) with vanes oriented at 25.4 mm spacing intervals as shown in Figure 3.1. The face and core layers were oriented in the same direction forming a unidirectional panel, and the face/core weight ratio was 50/50.

Figure 3.1 Mat formation process: forming box (left), and unconsolidated OSB mat (right)

A custom panel pressing profile (pressure and temperature) was created by InnoTech Alberta staff to manufacture samples with a uniform or flat vertical density profile (VDP). This approach was chosen to ensure that the unidirectional panels had a density distribution as homogeneous as possible both in-plane and out-of-plane. In order to achieve a flat VDP, a target of 5% w/w furnish moisture for the face layers and 7% w/w for the core layer were used. As shown in Figure 3.2, the panels were formed by hot pressing the loose (unconsolidated) mats using a hot oil heated press (Dieffenbacher North America Inc., Ontario, Canada) at 205°C for 380 s cycle (171, 174 and 35 s for close, cook, and degas stages, respectively).

Figure 3.2 Pressing process of the OSB panels: panels being pressed (left), and control system for pilot press system (right)

After the pressing stage, the panels had a nominal thickness of 15 mm, and were trimmed to 711 mm x 711 mm (28 x 28 in) to remove all rough edges. Final panel densities were obtained gravimetrically by weighing each panel and taking their average thickness. A total of 24 panels were manufactured which includes three replicates of four target densities (520, 560, 600, and 640 kg/m^3) and two wax loadings (0 and 2% wax content by weight). The target densities were chosen based on the upper and lower limit that could be produced based om the experience of the OSB pilot plant staff. These limits (and the increments in between) also represent the range of densities commonly found locally within commercial OSB panels.

3.2.2 Test specimen preparation

The manufactured panels were cut into two sets of specimens for characterizing: 1). moisture absorption (water immersion), and 2). vertical density profile (VDP). In total, 64 specimens were tested in this study to assess the effect of panel density (520 to 640 kg/m^3) and wax content (0 and 2% w/w based on oven dry weight). For the water immersion tests, square specimens were manufactured with dimensions 110 mm x 110 mm (4.33 x 4.33 in.), and were used to measure uptake of moisture over time which was used to determine the diffusivity constants (8 replicates per test condition). For the VDP assessment, a set of three specimens 50 mm x 50 mm (2 x 2 in.) were sampled from each panel produced to quantify the actual mean densities in each panel, and to validate the density uniformity through the thickness. The VDP were using an X-ray QMS Density Profiler QDP-01X (Tennessee, USA) located at InnoTech Alberta's wood composite panel pilot plant (Edmonton, Canada). All specimens were sanded before oven-drying at 105°C until a constant weight loss was achieved. After drying, the average thickness of each

specimen (measured on the four lateral faces) was measured to determine the actual mean densities.

3.2.3 Water immersion tests

In order to study the planar moisture absorption in the OSB specimens, the dried square specimens were sealed on both faces using three coats of an elastomeric sealant (Garland-white knight, Cleveland, OH, USA) followed by three coats of polyurethane (Rust-oleum-Varathane, Concord, ON, Canada) resin. In order to force the water diffusion in the x and y planes, the specimens were sealed on the top and bottom faces as shown in Figure 3.3 (i.e. two-dimensional moisture ingress from the edges only). After the coatings were applied, the sealed specimens were again put in an oven at 105°C to eliminate any residual moisture and to ensure coating curing.

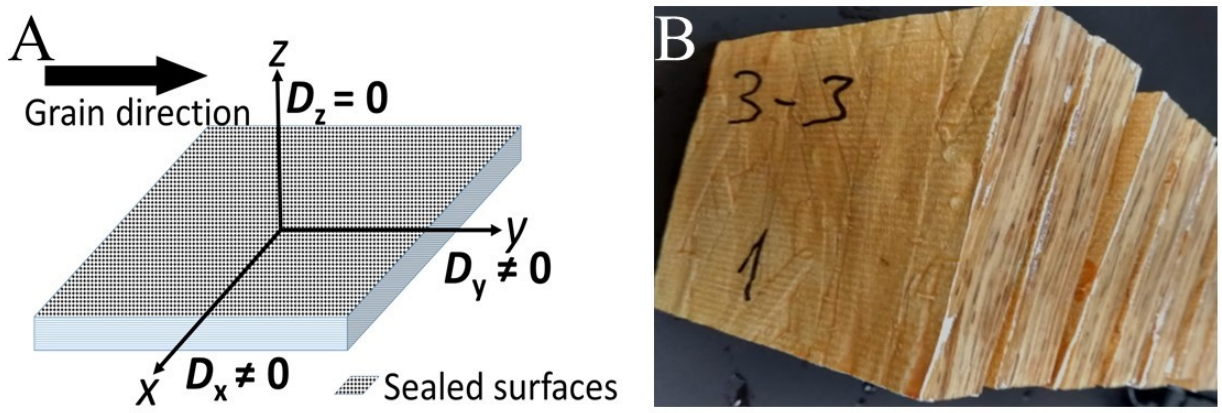

Figure 3.3 (A) Schematic representation of sealed specimens and their moisture diffusion directions in the *x* and *y* planes (B) actual photograph of sealed specimens

For the water absorption test, it was decided to completely submerge the samples in water (soak test) since wood composites panels are commonly subjected to short-term accelerated

soaking procedures for quality control purposes and for assessing product performance. In addition, this method has been widely used to study the effect of moisture on the dimensional stability and mechanical properties of OSB [69, 88–90]. Although this condition may be more severe than real ambient conditions, the intention of this procedure is to induce large moisture gradients which reach a level of saturation in a short time period.

The water absorption experiments were monitored gravimetrically where each specimen was fully immersed in distilled water at 20±1°C. At various time intervals, specimens were removed form the water bath and changes in mass were recorded using an analytical balance (Sartorius Entris 42021SUS, Göttingen, Germany) with 10 mg resolution. Prior to the mass measurement, excess of water on the surfaces of the specimen was wiped with a dry cloth, and the specimen was returned immediately to the water bath after weighing. Although it is not expected that an OSB panel has moisture content over 50% in actual practise, the mass measurements were taken up to the point of possible moisture saturation (i.e. plateau in mass gain) to have the necessary information for the determination of the diffusion parameters, and to have a better understanding of the failure mechanisms at high moisture content.

The moisture content on dry basis was determined according to the APA Performance Standard for Wood Structural Panel method [91]. The moisture content (MC) of the specimens at any given point in time was calculated using the following equation (Eq. 3.1):

$$MC = \frac{W_w - W_{s-dry}}{W_{dry}} \times 100 \quad (3.1)$$

where MC is the moisture content on dry basis over time (in %), W_w is the weight of the wet sealed specimen at a given time (in g), W_{s-dry} is the dry weight of the sealed specimen (in g), and W_{dry} is the oven dry weight of the specimen before be sealed (in g).

3.2.4 Analytical model for determining diffusivity constants

The diffusion of moisture in wood and wood-based products has been modeled using Fick's laws [67, 75, 77–80]. Fickian diffusion can be described by an initial stage where the slope is proportional to the water absorption of the material, followed by an asymptotic approximation to the maximum moisture content.

Fick's second law has been applied to describe the moisture concentration in anisotropic material as a function of time, which is described by the following equation (Eq. 3.2):

$$\frac{\partial C}{\partial t} = \frac{\partial}{\partial_x}\left(D_x \frac{\partial C}{\partial_x}\right) + \frac{\partial}{\partial_y}\left(D_y \frac{\partial C}{\partial_y}\right) + \frac{\partial}{\partial_z}\left(D_z \frac{\partial C}{\partial_z}\right) \quad (3.2)$$

where D represent the diffusivity coefficient (m^2/s) respect to the x, y and z (m) directions, C is the moisture concentration (kg/m^3), and t is time (s). Crank (Crank 1979) proposed an analytical

solution to Eq. (3.2) where the total weight gain as a function of time is determined by following expression (Eq. 3.3):

$$\frac{M_t}{M_{sat}} = 1 - \left(\frac{8}{\pi^2}\right)^3 \sum_{i=0}^{\infty}\sum_{j=0}^{\infty}\sum_{k=0}^{\infty} \frac{exp\left(-\pi^2 t\left(D_x\left(\frac{2i+1}{L}\right)^2 + D_y\left(\frac{2j+1}{l}\right)^2 + D_z\left(\frac{2k+1}{h}\right)^2\right)\right)}{\left((2i+1)(2j+1)(2k+1)\right)^2} \quad (3.3)$$

where M_{sat} is the saturation mass gain (kg), M_t is the mass gain (kg) as a function of time and L, l, and h (m) are the specimen dimensions. Later, Bao and Yee (Bao and Yee 2002) proposed an approximated solution to Eq. (3.3). The authors suggested that in the early stage of the absorption curve the weight gain by the specimen is the sum of the diffusion moisture in x, y, and z directions. Therefore, the initial weight uptake behavior is predicted by the following equation (Eq. 3.4):

$$\frac{M_t}{M_{sat}} = \sqrt{\frac{16t}{\pi}}\left(\frac{\sqrt{D_x}}{x} + \frac{\sqrt{D_y}}{y} + \frac{\sqrt{D_z}}{z}\right) \quad (3.4)$$

In order to identify the diffusion coefficient, the procedure proposed by Pierron et al [83] was used. The method builds up an objective function as shown in the following equation (Eq.3.5):

$$q = \sum_{i=1}^{n}\left(M_t(t_i) - M_i(t_i)\right)^2 \quad (3.5)$$

where $M_t(t_i)$ is the moisture content calculated from the analytical solutions at time t_i (Eq. 3.3), and $M_i(t_i)$ is the experimental moisture content calculated from the gravimetric curve at time t_i.

This method allows the determination of the best constants D_x, D_y, D_z, and M_{sat} that minimized the objective function, q, or quadratic error between the analytical solution and the experimental data points. Equation 3.5 was numerically solved using an *fmincon* function implemented in MATLAB R2019a.

3.2.5 Moisture diffusion simulations using finite element analysis

The moisture diffusion of a multi-layer, multi-directional OSB panel was simulated using a commercially available finite element software ANSYS (2020 R2). This software provides mass transport elements for moisture diffusion analysis, and can be used to model the moisture absorption behavior through the planar (x and y directions) of a non-homogenous OSB panel. The element used for moisture diffusion analysis was Solid 239 (20-node three-dimensional element) which offers moisture concentration as the degree of freedom at each node. The diffusion process implemented in ANSYS is governed by the second Fick's law that is expressed as (Eq. 3.6):

$$\frac{\partial C}{\partial t} = \nabla([D]\nabla C) - \nabla(\{v\}C) + G \tag{3.6}$$

where D is the diffusivity matrix, C moisture concentration, v the transport velocity vector, and G is the rate of diffusing substance generation per unit volume. The saturated concentration (CSAT) and diffusion coefficient (DXX, DYY, and DZZ) were input as material properties (MPDATA) and assigned to each element according to the element density. The initial boundary conditions of the model assumed a saturated condition as a degree-of-freedom constraint (D) at the external lateral nodes, while the initial concentration condition (IC) was zero for all internal nodes. The weight gain for each time step is calculated as a post-process step. The finite element (FE) model

determined the nodal values of the concentration gradient and diffusion flux from the integration point values. The total board weight gain is calculated by summing the individual mass contributions of each element, and the average moisture content for each specimen was calculated using Equation 3.1.

The developed finite element model based on Fick's law was used to predict the total moisture content of unidirectional OSB panels as a function of density and wax content, and to predict the moisture absorption profile (contour maps) in a commercial panel based on the unidirectional data set.

3.2.6 Immersion tests and analysis of moisture distribution in commercial OSB panels

Large-scale immersion tests were performed at InnoTech Alberta's lab (Edmonton, Canada) on two 305 mm x 305 mm (12 x 12 in.) specimens cut from commercial OSB panels using the same procedure outlined in section 3.2.3. The cut panels had average densities of 580 and 600 kg/m^3, and a nominal thickness of 18 mm. Similar to the small-scale tests, each cut panel was sealed at the top and bottom surfaces to ensure 2-D moisture transport in the plane of the panel (i.e. water ingress from the edges). During the water immersion tests, the samples were fully immersed in distilled water at 50 ± 1°C until an average moisture content of 42% (by weight) was achieved. During the test, the panels were removed at regular time intervals to perform two measurements: 1). weight gain to calculate the overall moisture content in the panel over time, and 2). 2-D moisture distribution scans in the specimens using a full field, X-ray tomography system to capture changes in the moisture profile over time. Weight gain was measured using a large analytical balance with a resolution of 10 mg, and moisture distribution was measured using a

custom ARC X-ray system (60 keV range) capable of scanning full-size sheets of wood composite panels.

For the X-ray measurements, moisture distribution in the specimens was analyzed based on the changes in intensity triggered by the presence of in-situ water. A baseline scan was taken of the oven dried (sealed) specimens prior to immersion which was also used to determine the average horizontal density distribution (HDD) over the entire panel surface. X-ray intensity maps (matrices) were obtained from the difference in intensity between the baseline and the wet samples at a given point in time. This difference was computed using a digital image processing software "ImageJ", and a digital representation of the moisture contours were generated and compared to the results from the finite element analysis.

3.3 Results and discussion

3.3.1 Vertical density profile (VDP)

The average VDP of three specimens cut from each manufactured panel (with and without wax) is shown in Figure 3.4 for each of the target average densities. To avoid overcrowded curves only one representative profile for each density and wax content is shown. The target and actual density for each manufactured panel is showed in Table 3.1, along with the actual measured (average) densities for VDP test specimens.

The VDP curves of each specimen type presents a reasonably uniform vertical distribution (Fig. 3.4A and 3.4B) which was obtained as a result of combined factors such as strand orientation, time and temperature during pressing, and strand furnish moisture content. The VDP for both un-waxed and waxed specimens shown a flat profile that is more uniform at low average densities (Fig. 3.4A and 3.4B).

Table 3.1 Target and actual density for each manufactured panel, and average measured densities for VDP specimens

Sample Id	Wax	Panel density		VDP Specimen	
		Target	Actual	Avg. density**	SD*
	(%)	(kg/m³)	(kg/m³)	(kg/m³)	-
A-1	0	520	526	523	89.4
A-2	0	520	523	561	53.8
A-3	0	520	517	511	30.0
B-1	0	560	559	543	60.7
B-2	0	560	564	573	42.9
B-3	0	560	564	543	71.2
C-1	0	600	598	585	69.3
C-2	0	600	609	608	40.8
C-3	0	600	600	689	17.0
D-1	0	640	634	673	54.5
D-2	0	640	644	678	26.2
D-3	0	640	645	685	63.6
E-1	2	520	520	469	41.0
E-2	2	520	520	514	28.4
E-3	2	520	520	526	77.3
F-1	2	560	563	629	52.4
F-2	2	560	563	630	33.7
F-3	2	560	562	602	32.0
G-1	2	600	600	598	46.9
G-2	2	600	602	686	19.5
G-3	2	600	603	642	22.1
H-1	2	620	622	595	36.8
H-2	2	620	618	604	54.5
H-3	2	620	613	654	20.8

* SD = Standard Deviation

** VDP sample density values are average of 3 samples taken from each panels

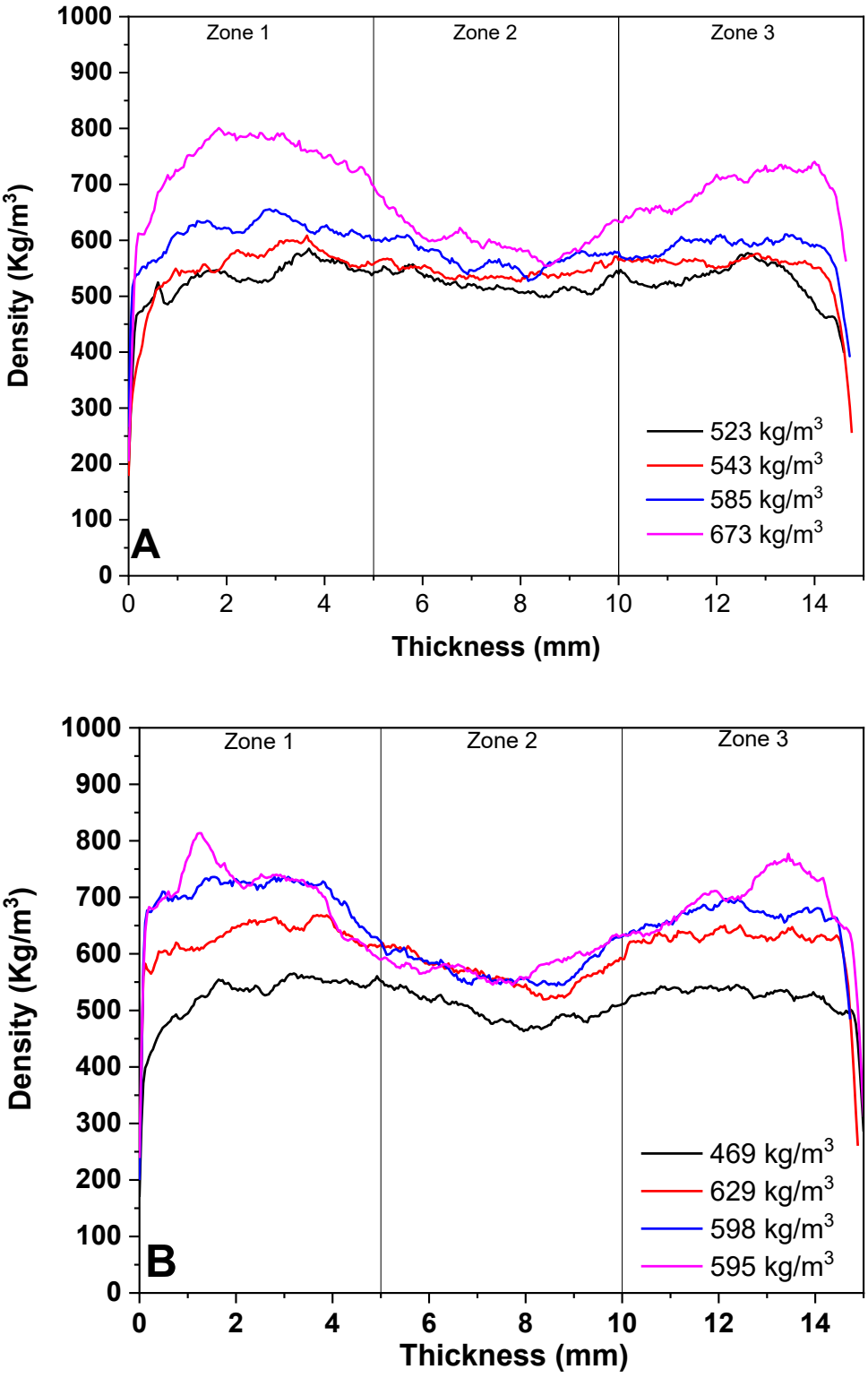

Figure 3.4 Representative vertical density profiles measured on OSB specimens for various actual density levels: (A) un-wax and (B) waxed specimens

3.3.2 Comprehensive water absorption curves

Figures 3.5 and 3.6 show specimen moisture absorption curves of both the un-waxed and waxed specimens for four different densities along the x and y directions as a function of water immersion time (in hours). All the specimens displayed a general shape where two different zones of water absorption are clear. The initial zone represents a classic Fickian behaviour with a rapid and linear weight uptake that was proportional to time. The un-waxed specimens had a faster water uptake compared to waxed specimens, as would be expected. In addition, the limit of linearity was different for the waxed *versus* un-waxed specimens. The linear portion of un-waxed specimen's response reached 60-70% of the final moisture content (MC) at 1.5 h (Fig. 3.5A) compared to 6-10% of MC at 4 h for waxed specimens (Fig. 3.5B). The second zone shows a non-linear response with a longer time period, and a slowing water absorption rate until the saturation (or equilibrium plateau) is reached. These results showed that the wax content affected the moisture absorption rate at both the initial and second zones of the curves (Fig. 3.6). It was observed that the water uptake rate (during the initial phase of moisture absorption) and total amount of moisture absorbed (at the plateau stage) both decreased with the addition of wax. For example, the MC% after 24 h of water immersion for un-waxed specimens reached over 90% for all the densities tested (Fig. 3.5A) whereas the MC% for waxed specimens reached a 23% and 14% at 523 and 619 kg/m^3, respectively (Fig. 3.5B). This is attributed to the hydrophobic nature of the wax which acts to reduce the availability of OH-groups present on the strands which limits interaction with the water molecules. These results agree with previous findings reported by Zhang et al [43]. In addition, the moisture absorption rate and weight uptake decrease with an increase in the density. Figure 3.5 and 3.6 show that the un-waxed and waxed specimens with higher densities presented slower water uptake rates in zone 1 of the curve and a reduced amount of water absorbed at the saturation stage.

For example, the water uptake absorption at 1.5 h for un-waxed specimens reached MC of 77% at 516 kg/m^3 and 40% at 638 kg/m^3 (Fig. 3.5A) compared to MC of 5% at 523 kg/m^3 and 3% at 619 kg/m^3 for waxed specimens (Fig. 3.5B). This may be explained by the compact structure of the board at higher densities as a result of greater strand-strand contact, thus reducing void spaces which reduces water molecule transport [92].

In addition, the MC% and water uptake rate for un-waxed specimens after reaching the linear absorption stage showed that the Fickian saturation stage was altered by zones with fast and abrupt increases in moisture uptake (see changes in slope after 50 hours in Fig. 3.6). Waxed samples presented similar behaviour, for example for high density samples at approximate 50, 75 and 130 hours of immersion the MC% present a faster water absorption rate (Fig 3.6). These initial changes in moisture absorption slope are most likely due to the releasing of compressive stresses during moisture exposure. In this process, high compaction forces from the hot press store potential energy in the panel thickness which is released when the panel is exposed to water. The release of this energy generated irreversible swelling allowing for further water ingress [93]. Longer-term abrupt changes in the moisture absorption curves are also likely related to the delamination effects at the panel edges due to the rupture of the adhesive bonds (see Figure 3.7) [41]. As moisture diffusion increases, swelling within the strands causes delamination effects at the edge of the specimen. This separation of layers, in turn, creates significant voids which further increase moisture uptake through capillary action. Additionally, the abrupt water absorption was more pronounced on waxed specimens, probably due to weak strand-to-strand bonding thus promoting a greater thickness swell [43].

Overall, the saturation or equilibrium plateau stage was influenced by wax content and density level (Fig. 3.6). The maximum moisture uptake decreased with an increase in the density

and with the presence of wax. For instance, the maximum MC% for un-waxed specimens reached 135% at 638 kg/m^3 compared to 160% at 516 kg/m^3 whereas waxed specimens reached 120% at 610 kg/m^3 compared to 135% at 523 kg/m^3 after 1000 h of water immersion. The lower maximum weight uptake of the specimens reached at higher densities indicate that it was more difficult for water molecules to penetrate the OSB internal structure. Furthermore, the lower saturation levels reached can be attributed to the addition of 2% wax (hydrophobic nature) that improved the water repellency and reduced the available surface area of water absorption of the specimens. These results agree with previous findings in the literature that the addition of wax and higher density reduces the maximum water uptake amount [43].

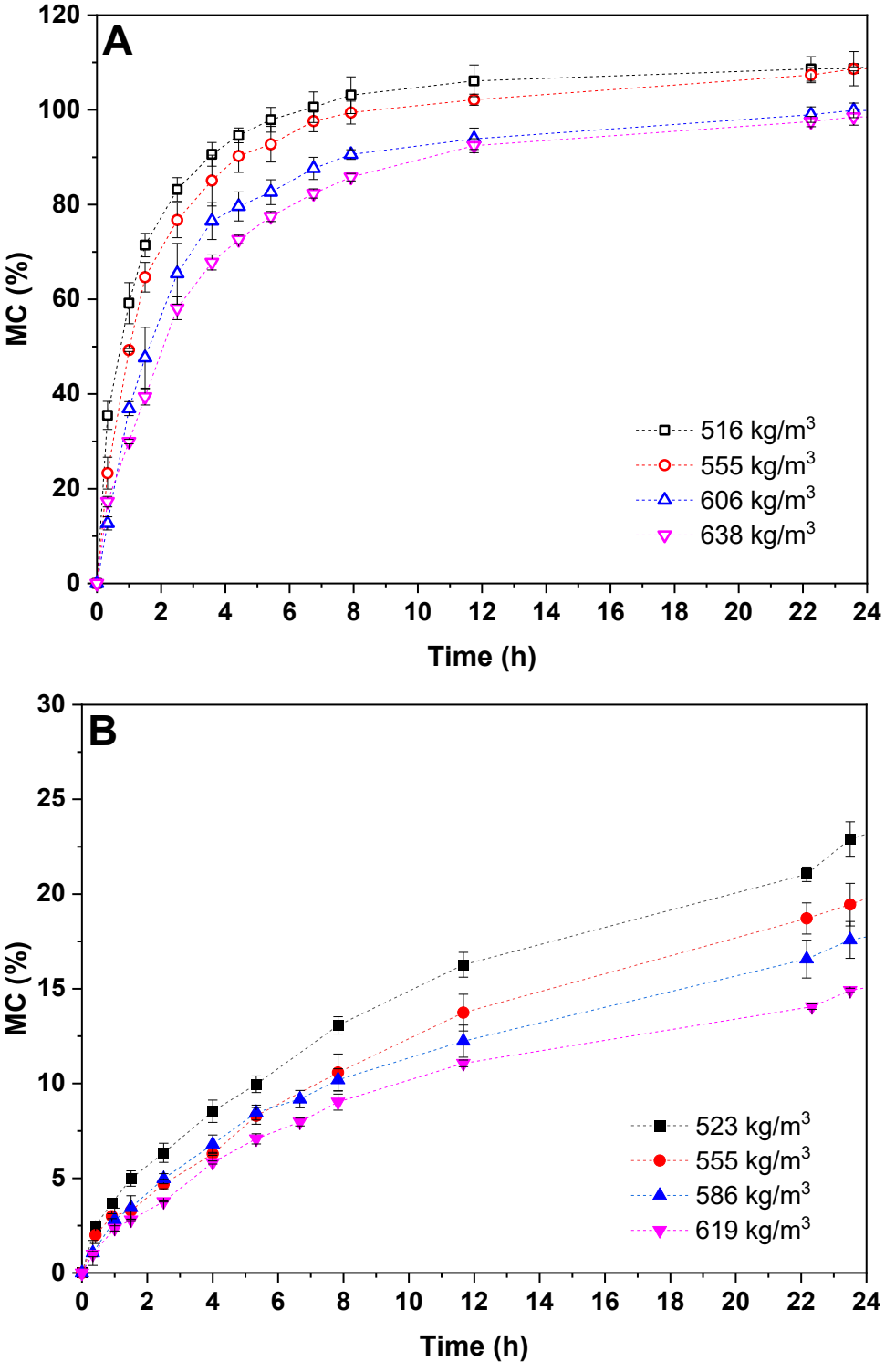

Figure 3.5 Short-term water absorption responses for un-waxed (A) and waxed (B) specimens up to 24 h of immersion time for various actual average panel densities. Error bar represent ± 1 std. dev.

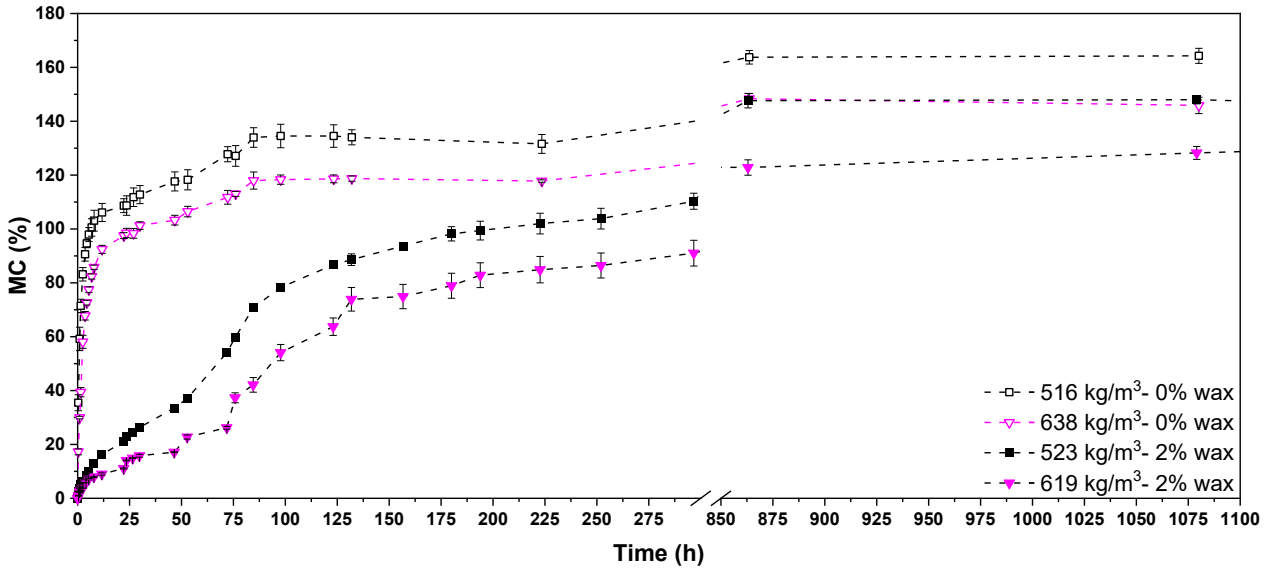

Figure 3.6 Long-term water absorption responses up to 1100 h for un-waxed (open symbols) and waxed (solid symbols) specimens. Error bar represent ± 1 std. dev.

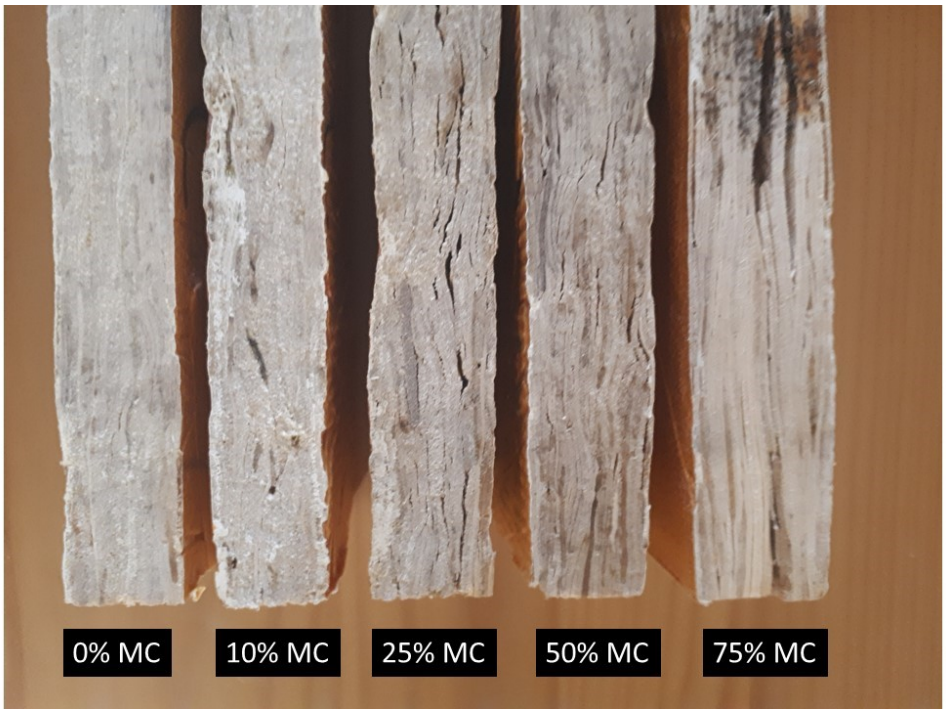

Figure 3.7 Swelling and delamination in OSB samples at various moisture content levels for panels density of 599 kg/m^3 (with 2% wax)

3.3.3 Diffusivity coefficients as a function of density and wax content

Moisture contents (%) as a function of the square root of immersion time for un-waxed and waxed unidirectional OSB specimens with different densities are illustrated in Fig. 3.8. In both figures (Fig. 3.8A and 3.8B), the curves displayed a Fickian behaviour with a linear stage in the initial moisture absorption process. The coefficient of determination for all fits were (Adj. R^2) ≥ 0.996. Liping and Deku [67] and Wu and Suchsland [78] have also reported that the mechanism of the water uptake process in wood-based composites followed a model described by Fick's law. From the results, it can be assumed that Fickian diffusion models may accurately describe the initial water absorption behaviour of OSB specimens. The linear stages (slope) of the moisture absorption curves was used to determine the diffusivity coefficients, specifically using a range of MC< 60% and MC< 30% for un-waxed and waxed specimens, respectively.

The diffusion coefficients, *D,* calculated from the experimental absorption curves of un-waxed and waxed specimens as a function of density and grain direction are presented in Fig. 3.9. The curves shown that the density, wax content, and strand directions of the specimens have a significant influence on the diffusivity constants. The diffusivity coefficient for un-waxed and waxed specimens increases linearly with a decrease in the density, as would be expected. The coefficients of determination (Adj. R^2) were ≥ 0.942 for all the linear curves. D_X for waxed specimens increased from 5.20×10^{-7} to 8.4×10^{-7} m^2/h when the density decreases from 619 to 523 kg/m^3 (Fig. 3.9B). This was due to the lower percentage of voids on the structure and the higher number of strands compacted on the structure with higher density panel, thereby generating a physical barrier that difficult the easy migration of water on the specimen. These observations are similar to the results of Dai and Yu, [94] who stated that the water absorption of OSB is influenced by the presence of voids between strands. Xu and Winistorfer [95] and Chen et al [12]

also reported that the moisture diffusivity on boards with a low-density absorbed moisture faster than boards with high-density. Also, Wu and Suchsland [53] reported that particleboard with lower density (core layer) shown larger moisture diffusivity than the surface layer.

Figure 3.9 shows that the diffusivity coefficient of OSB specimens was also affected by wax content. As expected, the addition of wax increases the hydrophobicity of the boards by reducing the surface energy which is reflected in the dramatic decrease of the diffusivity coefficient. The *D* values at 2% of wax content are three orders of magnitude lower compared to those at 0% of wax content for the range of density studied. For instance, the *D* values at 635 kg/m^3 for waxed specimens were 4.90×10^{-7} and 8.20×10^{-7}m^2/h compared to $1.02 \times 10^{-4}$and 1.76×10^{-4} m^2/h of those un-waxed specimens at *x* and *y* directions, respectively. These findings confirmed that wax acts as a water repellent and can reduce the diffusion/absorption of water on OSB panels [31].

The diffusion coefficient, *D,* of strands with the perpendicular grain direction (*x*-direction) of un-waxed and waxed specimens was significantly lower than those strands with parallel to grain direction (*y*-direction). It was approximately 38% lower along the perpendicular to the grain direction than that along the parallel to the grain direction. However, the difference in diffusion coefficient between both directions is smaller as the density increases. For example, the percentage of difference of the diffusivity coefficient in *x* and *y* directions for un-waxed specimens increases in about 41% and 39% when the density decreased from 638 to 516 kg/m^3 (Fig. 3.9A) while waxed specimens, it increases in about 38% and 34% when the density decreased from 619 to 523 kg/m^3, respectively (Fig. 3.9B). A similar trend was reported by Zhang et al [43], who found differences in water absorption as a function of wood strand direction. This can be attributed to the long-cell microstructure along the grain direction of the wood. Along this grain direction, water is more

easily absorbed and transported through the wood relative to moisture absorption perpendicular to the grain direction. Furthermore, higher densification of the structure can impede the water absorption process [57, 81].

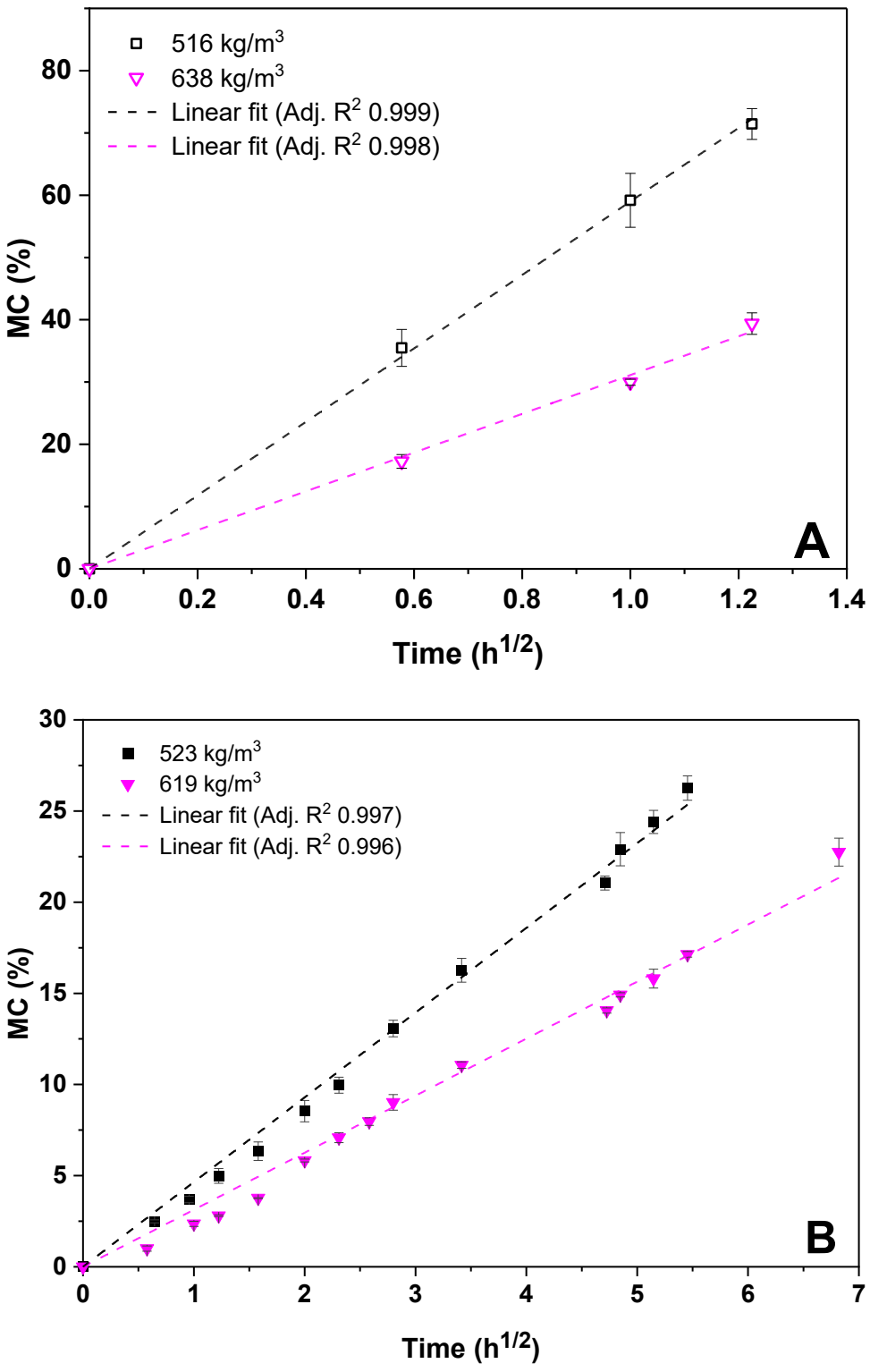

Figure 3.8 Moisture content (%) as a function of the square the root of immersion time: up to 1.4 $h^{1/2}$ for un-waxed (A) and 7 $h^{1/2}$ for waxed specimens (B). Error bar represent ± 1 std. dev.

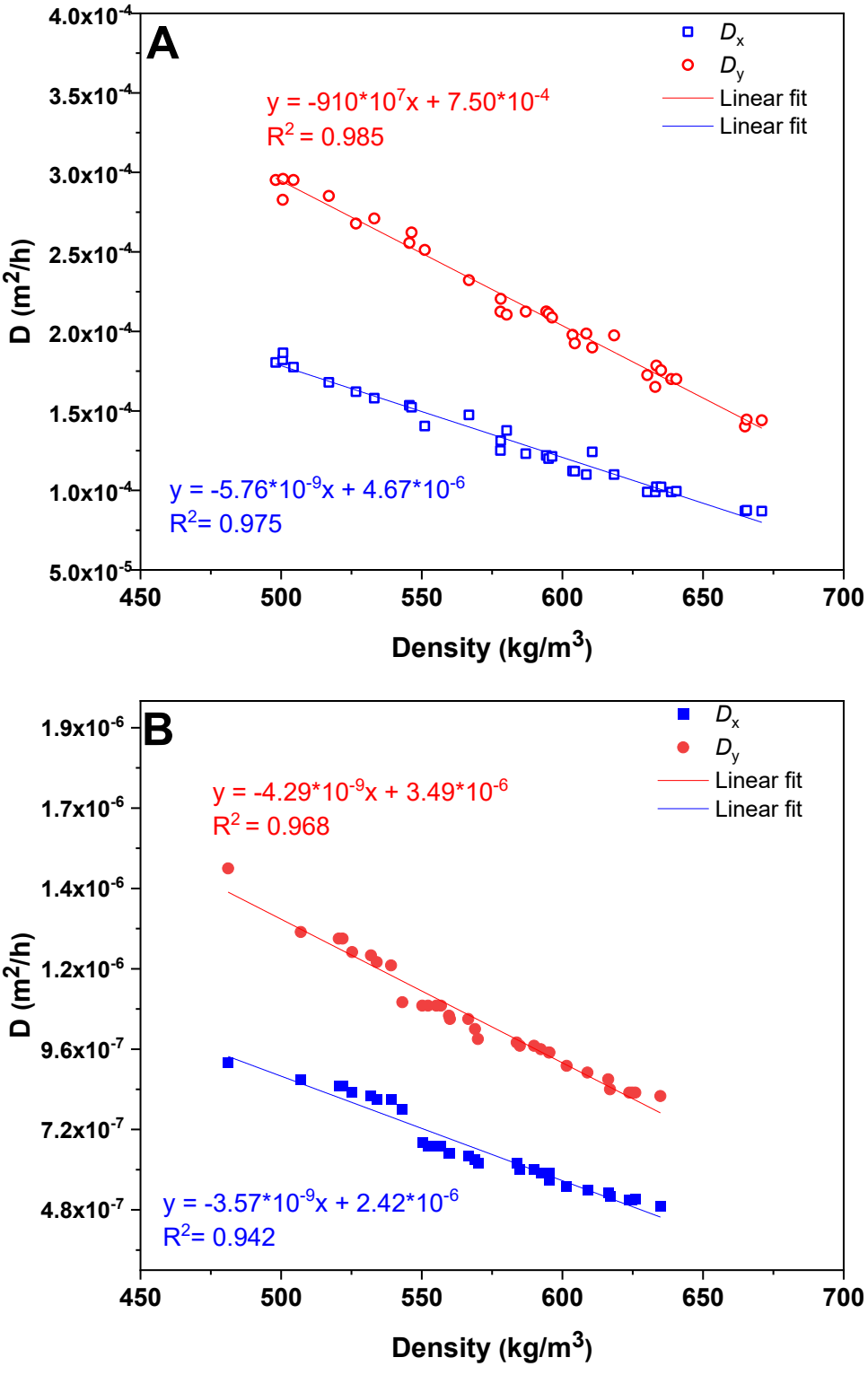

Figure 3.9 Fickian diffusion coefficient displayed as a function of density levels and grain direction (x and y directions) for un-waxed (A) and waxed specimens (B)

3.3.4 Prediction of moisture absorption using finite element methods

The developed finite element model based on Fick's law was used to predict the total moisture content of unidirectional as a function of density and wax content. Table 3.2 summarizes the diffusion parameters of un-waxed and waxed specimens estimated from the linear fit analytical solution (Fig. 3.9) used as inputs to the finite element model.

Fig. 3.10 shows a comparison between the experimental and simulated curves of moisture gain over time. As shown in the figure, the finite element model does a good job of predicting the overall diffusion behaviour of the experimental data. The global relative error (e) [96] was used to compare the average MC measured for each specimen and that predicted by the model as:

$$e = \frac{\sqrt{\sum_{i=1}^{N}\left[MC_{exp}(t_i) - MC_{pred}(t_i)\right]^2}}{\sqrt{\left(\sum_{i=1}^{N} MC_{pred}(t_i)\right)^2}} \times 100 \tag{3.7}$$

The best agreement between the MC% of specimens and that predicted by the model for the OSB specimens tested occurred at the beginning of the absorption process. For example, the global relative error, e, for un-waxed specimens between 0 to 24 h of moisture absorption were only 1.2, 1.7, 2.2, and 1.9% at densities of 516, 555, 606, and 638 kg/m^3, respectively. A similar trend was also shown for waxed specimens for immersion times between 0 to 46 h. Error values for these samples were 1.8, 2.0, 4.0, and 3.1% at densities of 520, 550, 585, and 620 kg/m^3, respectively. At longer time periods, the difference between the model and experiments is seen to increase. Fig. 3.10 shown a systematic error between experimental curves and that predicted by the model after 24 and 30 h of immersion for un-waxed and waxed specimens, respectively. As a result, the Fickian diffusion model is not sufficient for predicting the absorption process for

prolonged immersion times. For these cases, a dual-stage absorption model may need to be introduced.

The deviation between MC% predicted by the model and MC% measured experimentally were quantified by linear regression. As shown in Fig. 3.11 and Table 3.3, the MC% predicted by the model indicates a strong linear relationship with a good agreement with the MC% measured (Adj. $R^2 \geq 0.981$) for un-waxed and waxed specimens for all densities tested.

The deviations between the MC% predicted by the model and measured were higher over at MC $\geq$ 100% in Figure 3.11A, and 25-30% of MC for un-waxed and waxed specimens, respectively. At these levels of MC%, the model tended to predict lower weight gain than experimental data. As discussed previously, the abrupt weight gains can be attributed to excessive swelling which was observed during the tests, and is associated with non-Fickian behaviour. Unfortunately, the finite element model FEM is only based on Fick's diffusion equation, and does not consider the water potential or capillary action [97]. Thickness swell ultimately creates new empty spaces and causes changes in the shape of pores [98]. These microstructural changes are not considered by Fick's diffusion equation.

As a final step, the finite element model was also used to predict moisture absorption behaviour in a commercial (multi-directional) OSB panel. These predictions were based on the diffusivity coefficients derived from the unidirectional OSB experiments (see Table 3.2), and the results were compared to moisture penetration profiles (contours) determined experimentally from a limited set of 18 mm (23/32 in) three-layer commercial panels (i.e. strands in the core layer were perpendicular to the strands on the faces). In order to validate the moisture distribution predicted by the model, the difference in the intensity between dry and wet specimens obtained by X-ray scans at different MC% were compared with the predicted contours obtained by the model. The

moisture content gradients in the commercial OSB were determined by considering the horizontal density distribution of the specimen obtained by X-ray. The diffusivity coefficient and saturation levels as function of horizontal density distribution was assigned to each individual element. A qualitative comparison between predicted and the experimental moisture contours are shown in Figure 3.12.

The images on the left represent the moisture profile changes based on X-ray normalized intensity at three different moisture contents while the right figures represent the normalized ratio between the concentration of saturation and the concentration of each node at the same moisture content (Fig. 3.12). For both the experimental and model contour plots, it can be seen that the highest moisture concentration starts at the exposed edges of the panel and progresses inward over time. In general, the moisture contours in the experimental images are less homogeneous than the simulated contours from the finite element model. This is likely due to local inhomogeneities and variations in the actual physical panel that are not accounted in the model (e.g., void, gaps or vertical density variations). However, the X-ray results do show definite utility in indirectly characterizing the moisture distribution in an OSB panel [99]. The qualitative comparison confirms that the model not only capable of predicting the total MC changes but it also shows a reasonable estimate of moisture gradients throughout the OSB panels.

Table 3.2 Diffusivity parameters of un-waxed and waxed specimens determined from the linear fit analytical solution

Un-waxed specimens				Waxed specimens			
Density kg/m^3	D_x m^2/h	D_y m^2/h	M_{sat} %	**Density** kg/m^3	D_x m^2/h	D_y m^2/h	M_{sat} %
516	1.63×10^{-4}	2.78×10^{-4}	109	523	8.08×10^{-7}	1.25×10^{-6}	113
555	1.40×10^{-4}	2.43×10^{-4}	105	555	7.08×10^{-7}	1.11×10^{-6}	103
606	1.11×10^{-4}	1.96×10^{-4}	101	586	6.12×10^{-7}	9.76×10^{-7}	95
638	9.25×10^{-5}	1.67×10^{-4}	98	619	5.09×10^{-7}	8.34×10^{-7}	85

* Actual average density

Table 3.3 Regression parameters for un-waxed and waxed specimens

Un-waxed specimens				Waxed specimens			
Density* (kg/m^3)	**Adj. R^2**	**Slope**	**Intercept**	**Density*** (kg/m^3)	**Adj. R^2**	**Slope**	**Intercept**
516	0.990	0.984	0.107	523	0.989	0.9321	1.008
555	0.987	0.926	5.060	555	0.994	0.8972	1.735
606	0.981	0.911	8.615	586	0.994	0.9056	0.631
638	0.988	0.902	8.119	619	0.990	0.8372	1.048

* Actual average density

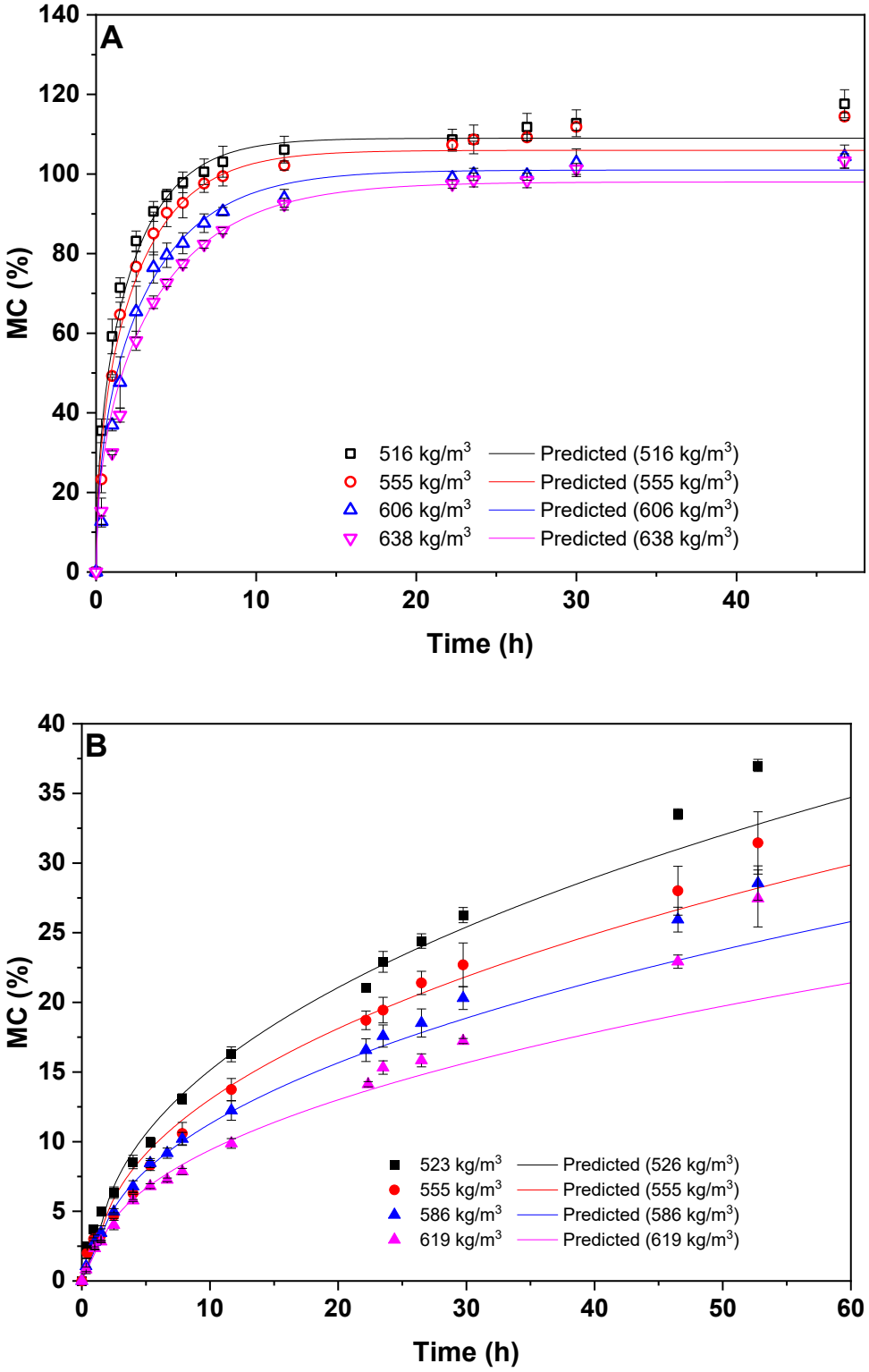

Figure 3.10 Experimental water uptake curves (symbols) of un-waxed (A) and waxed (B) specimens compared with FEM simulated curves (lines) as a function of water immersion time. Error bar represent ± 1 std. dev.

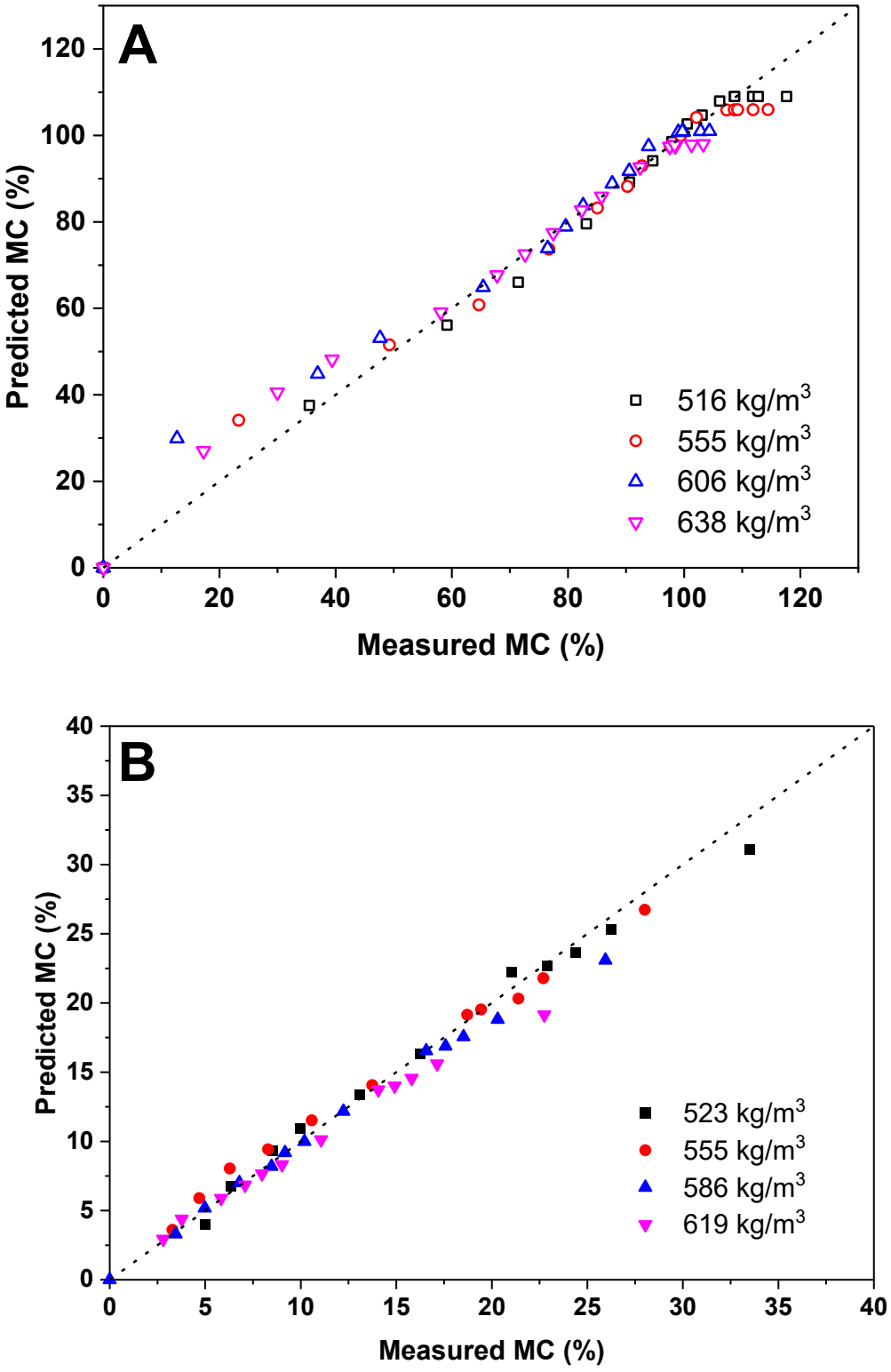

Figure 3.11 MC% predicted by the model *versus* MC% for un-waxed (A) and waxed (B) specimens at different densities

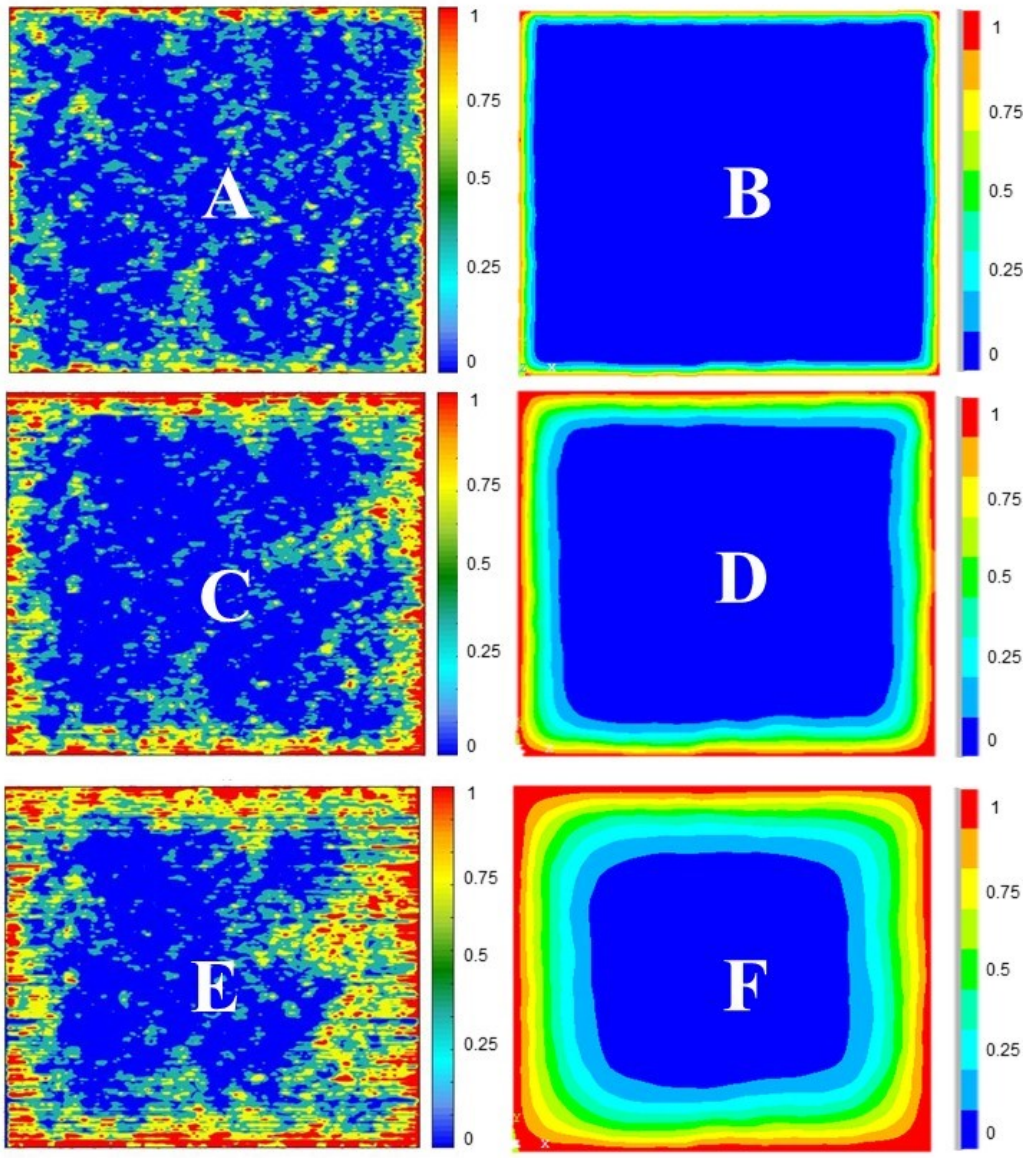

Figure 3.12 Predicted moisture profiles (normalized) across commercial panels for average moisture contents of 11% (A-B), 25% (C-D), and 42% (E- F) where the left graphs are the experimental X-ray intensities, and the right graphs are concentration gradients from the finite element model

3.4 Conclusions

This study shows that a finite element model based on Fick's second law fits the experimental data accurately at the first stages of the moisture absorption process on OSB panels. The moisture transport parameters were empirically determined by fitting experimental weight gain data with an analytical solution.

The weight gains curves of unidirectional un-waxed and waxed OSB specimens with a flat VDP were immersed in water at room temperature to obtain the moisture transport parameters of the constituent layers of the sample. It was found that moisture absorption and diffusivity coefficients of OSB specimens depended on the density, grain direction, and wax content. Both increased panel density and the introduction of wax content had significant effects reducing the amount and rate of water uptake. In addition, the diffusivity coefficient was found to be lower along the perpendicular-to-grain direction than to the parallel-to-grain direction.

By comparing the predicted results with the experimental data, a strong linear relationship (Adj. $R^2 \geq 0.994$) was obtained in this study. As a result, the developed finite element model was found to be a useful tool to predict and describe the process of moisture absorption in commercial OSB panels. Some improvements to this simple model are proposed as future work. This includes a better understanding of the actual diffusivity mechanisms and the microstructural features of the internal matrix, and the effect of dimensional changes resulting from swelling.

Chapter 4: Effect of moisture absorption on the bending properties of oriented strand board

4.1 Introduction

Currently, the demand within the construction industry for Oriented Strand Boards (OSB) composites used as wall and roof sheathing, flooring, and packaging has increased significantly and continues to grow [2]. As a result, there is a need to better understand and tailor board properties to manufacture high-quality products for both existing and new applications. In particular, understanding product durability and performance under adverse conditions is crucial, especially with respect to degradation of structural properties such as strength and stiffness.

One of the main challenges facing OSB (and other wood-based products) is moisture absorption which can result in physical/dimensional changes (e.g., thickness swell), and reduction in mechanical properties (e.g., stiffness, flexural strength and internal bond strength) [86]. Protection from wet environments is the most common approach to mitigate moisture in OSB, and includes coverage of panels with impermeable construction materials such as polymer films, paints, siding/stucco for exterior walls, or shingles in roofing applications. Even with these mitigation strategies, wood composites can still be susceptible to moisture ingress during shipping/storage and as a result of improper construction practices.

To better understand this problem, there has been significant research over the past few decades investigating the effects of moisture on OSB and its properties. Several studies have reported that moisture absorption in OSB can affect dimensional stability (e.g., thickness swell) and mechanical performance which ultimately can reduce the service life [7, 34, 49, 50, 52, 54, 87, 88]. Furthermore, water uptake in OSB (e.g., moisture absorption rate) has also been well studied, and has been found to be affected by many factors including strand geometry, wood

species, density profile, manufacturing parameters, resin type and content, and wax content [89–92].

While there is significant experimental data available in the literature on OSB, translation of these findings into useful models or tools for analysis and improvement of OSB (and other wood composites) is somewhat limited. This is primarily due to the heterogeneity and complexity of OSB's structure at both the macro- and micro-scales. In terms of modeling approaches, both empirical and numerical models have been developed to predict the behaviour of OSB and wood composites under different scenarios. However, relatively few studies have been focused on modeling and predicting the effects of key OSB parameters such as board density, grain orientation, wax content, and moisture content on the mechanical properties of engineered wood composites. In terms of empirical approaches, Chen et al [51] used linear and quadratic regression to investigate the relationship between major properties (MOR, MOE, IB, TS and rolling shear strength) of multidirectional OSB panels as a function of panel density (449 to 705 kg/m^3). The authors found that MOE and MOR increased with increasing panel density, while TS and water absorption decreased. Moreover, they reported that OSB panels with higher densities absorbed water more slowly, reducing the rate of TS. Barnes [10, 38, 39] developed an empirical model that predicted tensile strength, MOR, and MOE. The author concluded that increasing strands length improved the OSB bending properties. Barbuta et al [22] determined the regression equations to predict the unidirectional strand board mechanical properties as a function of density (550, 700, and 850 kg/m^3) and moisture content (20 and 50% RH at 20°C). The results indicated that the mechanical properties of the panels improved as panel density increased, however, relative humidity did not have a significant effect on mechanical properties

Despite these research efforts, the relationship between mechanical performance and local moisture content of OSB is still unclear. As a result, more studies are required to better understand and capture these effects with empirical models. Once developed, these empirical models can be used directly by manufacturers and the engineering community to assess moisture effects in OSB, and can also be used as critical input for more complex models such as finite element approaches.

The main objective of this study is to investigate the relationship between bending strength/stiffness and moisture content for unidirectional OSB specimens (with a uniform/flat vertical density profile) as a function of grain direction, board density, and wax content. The intent is to provide essential information that will be fundamental to the development of future models, and to build on existing models (both empirical and numeric) developed by the author which can predict moisture absorption rates and profiles in OSB as a function of board density, grain direction and wax content (refer to Chapter 3). These models could ultimately be used to better understand the mechanisms of dimensional stability in OSB (e.g., thickness swell), and for use in designing long-term, stable engineered wood composites.

4.2 Materials and methods

4.2.1 Materials and manufacturing process

Unidirectional OSB panels were manufactured at InnoTech Alberta's wood composite panel pilot plant (Edmonton, Canada). All the panels were manufactured with commercial Aspen strands of an average of 0.86 mm thickness and 108 mm length obtained from a local OSB mill. The fines were removed using a 4.76 mm deck screen to minimize their influence in the furnish. OSB boards with dimensions 865 mm in length (34 in) by 865 mm in width (34 in) and 15 mm in thickness (19/32 in) were produced. Strands were blended with 3.5% w/w (based on oven dry

weight) commercial liquid phenol-formaldehyde (Hexiom PrimaxTM AB17A6H, 48% of solids) for both the face and core layers. In addition, two wax contents were considered: 0% (no wax) and 2% w/w (based on oven dry weight) of E-wax Slack (Hexion EW58S, 58% of solids). In order to achieve a flat or uniform vertical density profile (VDP), a target of 5% w/w furnish moisture content for face and 7% w/w moisture content for core layer were used. The strands in the face and core layers were oriented in the same direction, and the face-to-core weight ratio was 50:50. All mats were formed by hand employing a forming box (865 mm x 865 mm) with a vane orienter of 25.4 mm (1.0 in). Panels were pressed using a hot oil heated press (Dieffenbacher North America Inc., Ontario, Canada) which allows for monitoring of mat pressure and thickness, core temperature and gas pressure. A series of panels with four target densities were produced as shown in Table 3.1. Once pressed, the OSB panels were trimmed to a final dimension of 711 mm (28 in) x 711 mm (28 in) to remove the rough edges. The final actual panel densities were obtained by measuring the panel weight and final dimensions after the pressing and trimming stages. A total of 24 panels were produced which include 4 density variations, 2 wax contents (no wax and 2% w/w), and 3 replicates per test condition

4.2.2 Specimen preparation

The manufactured unidirectional panels were cut into rectangular shaped bend test specimens with dimensions 350 mm (13.75 in.) x 50 mm (2 in.) with both parallel and perpendicular grain orientations. Three different parameters were tested in this study, which included: panel density, wax content (0 and 2% w/w), and grain direction (parallel and perpendicular). In total, 457 test specimens were manufactured of which 224 specimens were parallel to the grain direction, and 233 were perpendicular to the grain direction. Before testing,

all specimens were sanded and then oven-dried at 105°C until they reached constant weight. After drying, the average thickness of each specimen was measured at 6 points using a micrometer. All specimens were sealed at the top and bottom surfaces using the procedure presented in Chapter 3 (Section 3.2.3).

4.2.3 Bending tests

Prior to mechanical testing, bend (flexural) specimens were conditioned to one of five target moisture contents: 0, 10, 25, 50 and 80% (based on oven dry weight). Each specimen, was fully immersed in distilled water at 20±1°C, and the mass gain was measured over time using an analytical balance (Sartorius Entris 42021SUS, Göttingen, Germany) with 10 mg resolution. In addition to the mass, the average thickness at each time period was also measured based on 6 readings for each specimen. The moisture content (MC) at any given time was then determined using Equation 3.1 (see Section 3.2.3). For each target MC, a set of bending specimens was selected in order to have a similar density within each group (for data plotting purposes).

Once the target MC was achieved, three-point static bending tests were performed on all samples according to ISO 16978 (International Standard - Wood-based panels - Determination of modulus of elasticity in bending and of bending strength). Tests were conducted using an Instron universal testing machine (Norwood, USA) equipped with a 10 kN load cell (Interface, SSM-AJ-200, USA). The test span was 300 mm, and the loading rate was set at 250 mm/min for all the experiments.

To calculate the flexural properties of the specimens, thickness values were measured after moisture exposure and a fixed span of 300 mm and width of 50 mm for all the MC levels was used.

The modulus of elasticity (MOE) and bending strength or modulus of rupture (MOR) of each specimen was calculated using the following equations:

$$MOE = \frac{{l_i}^3(F_2 - F_1)}{4bt^3(a_2 - a_1)} \tag{4.1}$$

$$MOR = \frac{3F_{max}l_i}{2bt^2} \tag{4.2}$$

where l_i is the distance between the centres of the supports (mm), b is the width of the test specimen (mm); t is the thickness of the test specimen (mm) at target MC (based on oven dry weight), $(F_2 - F_1)$ is the increment of load on the straight-line portion of the load-deflection curve (N); $(a_2 - a_1)$ is the increment of deflection at the corresponding force (mm), and F_{max} is the maximum load (N).

4.2.4 Thickness swell measurements and calculation

The thickness swell (TS) of each rectangular sealed specimen was measured with a digital micrometer caliper at six locations on the four edges (two on the short edges and 4 on the long edges) to obtain the average specimen thickness. The TS of the specimens (in %) was calculated using the following equation:

$$TS = \frac{(T_t - T_0)}{T_0} \times 100 \tag{4.3}$$

where T_0 is the average of the six oven-drying thickness measurements (mm) and T_t is the average of the six thickness measurements at different times. The same location on the specimen was used for each of the TS measurements.

4.2.5 Experimental statistical analysis

Statistical analysis of data was performed using RStudio statistical software (Version 1.1.383). A linear fit was performed on each dataset, and an analysis of variance (ANOVA) was performed on each lineal model with a 95% confidence interval (to confirm the significance of the various parameters tested).

4.3 Results and discussion

4.3.1 Thickness swell as a function of density, wax content, and strand orientation

Thickness swell (%) as a function of density for un-waxed and waxed unidirectional OSB specimens with different strand orientations are provided in Fig. 4.1. In addition, the results of the ANOVA for the regression analysis on the impact of board density, wax content, and grain orientation on the TS of OSB specimens as a function of the different average MC% are presented in Table 4.1.

In both figures (Fig. 4.1A and 4.1B), the TS can be seen to increase linearly with increasing specimen density. The slope of this linear relation between TS and density, however, is affected by MC (i.e. slope increases with MC). For example, at 10% MC, TS increased from 2.9 to 3.6% (approx. 1.2 times increase) when the density increased from 495 kg/m^3 to 666 kg/m^3, while at 80% MC, TS increased from 21 to 38.5% (approx. 1.8 times increase) when the density increased from 501 kg/m^3 to 655 kg/m^3 (Fig. 4.1B). Similar trends were observed on all the conditions tested. The resulting statistical analysis showed a strong relationship (at a 5% significance level) between TS and density for un-waxed and waxed OSB specimens along parallel and perpendicular directions for all the MC tested. The TS effect is caused by two mechanisms: a) the swelling of

wood itself, and b) the swelling developed from the release of compression in the mat [100]. Therefore, higher density panels contain more individual strands that may contribute to the total swelling. In addition, higher density panels have lower moisture diffusivities (as discussed in Chapter 3) resulting in longer exposure times required to reach the target MC which may lead to increased swelling behavior. These results are in agreement with Wu and Piao [8] and Geimer [101] who reported that TS or TS rate (i.e. TS divided by total water absorbed) increases with increasing specimen density.

While panel density was observed to play a role in TS, the addition of wax did not show a significant effect on TS at equivalent average MC levels (a confirmed by the statistical analysis in Table 4.1). This is contrary to other studies which found that wax content reduced thickness swell [41]. However, these studies only measured TS at fixed points in time rather than at total moisture content levels. This suggests that the addition of wax only slows down the TS effect, but does not eliminate it. Furthermore, these results corroborate the moisture absorption findings in Chapter 3 which show that waxed specimens had lower diffusivity values (i.e. lower moisture diffusion rates), but had similar overall moisture uptake to unwaxed specimens, particularly at high average moisture content values.

In terms of grain direction, there is a small observed difference between specimen grain direction (parallel *versus* perpendicular specimens) on TS measurements particularly at lower MC values (see Table 4.1). The ANOVA test indicates that grain orientation was slightly significant at 10% MC (Pr = 0.047) and significant at 25% MC (Pr = 0.00004). However, at the higher MC levels (50% and 80%), the effect of strand orientation on TS was not significant. This suggests that moisture ingress at the two long edges *versus* the two short edges of the rectangular specimen may play a role at these lower MC values. It is known that moisture transport along the wood grain is

easier/faster than transport perpendicular to the grain direction, and is due to the natural lumen (hollow) microstructure in wood which occurs in the grain direction [102]. As such, specimen edges with cuts perpendicular to the lumen microstructure (i.e., perpendicular to the grain) should provide more accessible pathways for moisture to enter the panel compared to edges parallel to the grain.

Table 4.1 Results of the analysis of variance (F and P values) for linear fit of TS% as function of density board, wax, and orientation at different MC levels

MC	Factor	F Value	Pr(>|F|)
10%	Density	8.395	0.00467**
	Wax	0.144	0.70544 NS
	Orientation	4.038	0.04735*
25%	Density	44.259	1.959×10^{-09}***
	Wax	0.1626	0.68774 NS
	Orientation	13.670	0.00004***
50%	Density	91.333	1.132×10^{-15}***
	Wax	3.578	0.06201 NS
	Orientation	0.280	0.16205 NS
80%	Density	140.625	$<2 \times 10^{-16}$***
	Wax	2.074	0.1554 NS
	Orientation	0.122	0.7282 NS

***: Significant at [0, 0.001] probability level
**: Significant at (0.001, 0.01] probability level
*: Significant at (0.01, 0.05] probability level
NS: Not significant at (0.05, 1] probability level

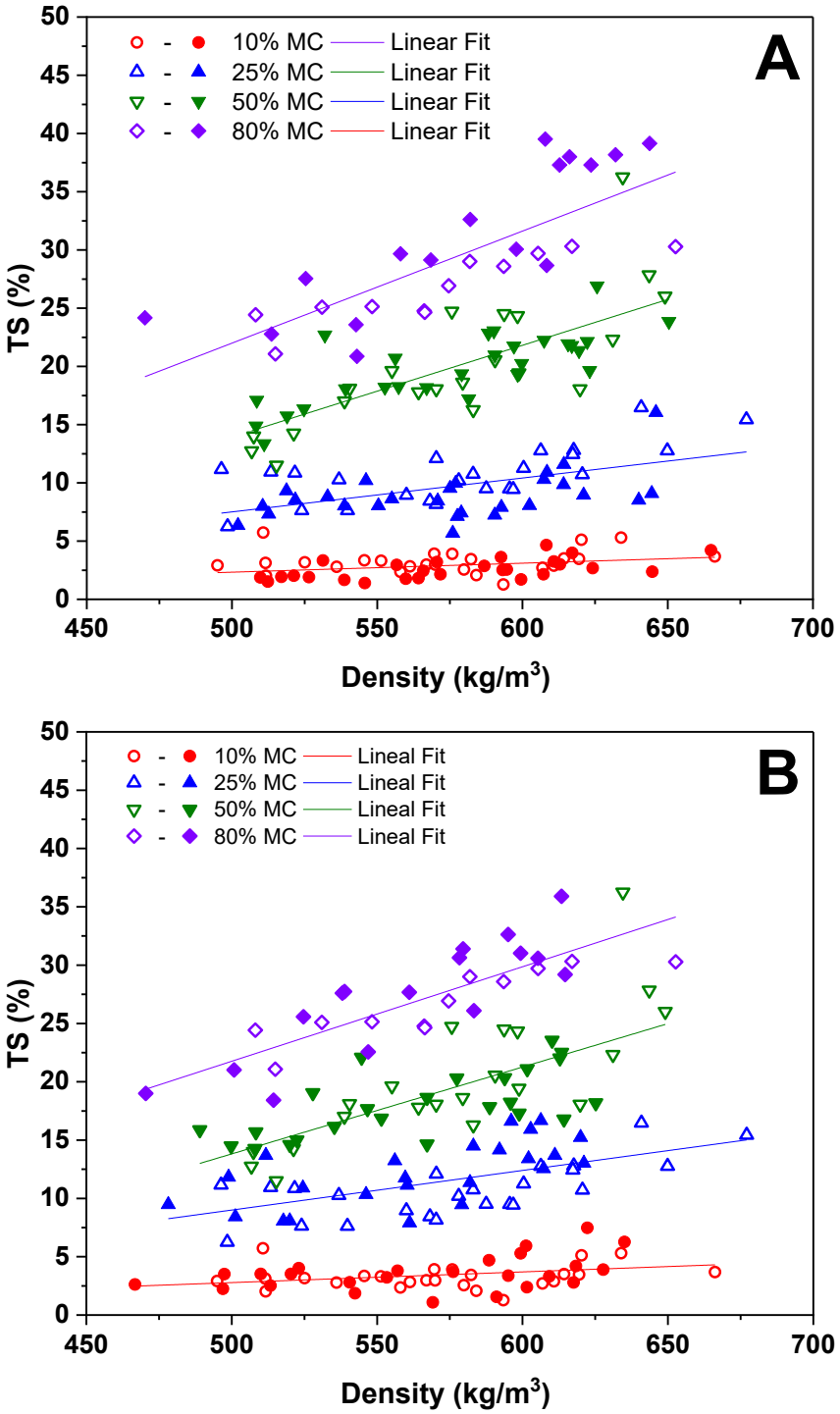

Figure 4.1 Thickness swell (TS) results (in %) as a function of specimen density for parallel (A) and perpendicular (B) specimens at different densities for un-waxed (clear symbol) and waxed (solid symbol) specimens

4.3.2 Effect of wax content, grain direction, panel density, and MC level on bending strength and stiffness

The relationships between MOE/MOR, density, grain directions, and wax content at five average MC levels (0, 10 25, 50, and 80% based on oven-dry weight) of the specimens tested are plotted in Fig. 4.2 to 4.5. The results of the VDP for these specimens were presented in Chapter 3 (Section 3.3.1).

Overall, the mechanical properties (MOE and MOR) of the unidirectional OSB specimens tested were affected by moisture content (MC), panel density, and strand grain orientation. Moisture content is a predominant factor in both MOE and MOR degradation. For all conditions, an increase in average MC results in a decrease in both MOE and MOR. This decrease is seen to be most dramatic at lower MC levels, and seems to level off (plateau) at the higher MC values. These results corroborate findings from previous studies on multidirectional OSB panels [58, 103, 104]. This reduction in MOE and MOR due to moisture can be attributed to the degradation of the wood constituents such as cellulose and hemi-cellulose (e.g., weakening or breaking of the hydrogen bonds between different polymer chains in the crystalline cellulose microfibrils) which results in reduced microstructural bonding [105]. At higher moisture contents, macroscopic damage modes such as cell wall expansion, cracking and delamination can also occur due to moisture swelling effects which also affect mechanical properties [56].

The experimental results also indicate that there is a clear difference of MOE or MOR trends attributed to the strand grain direction (parallel *versus* perpendicular). The difference decreased with increasing MC content, suggesting that MC is a predominant factor on bending properties in the two directions. The impact of grain directions on bending properties of the unidirectional OSB specimens can be observed by the differences in MOE or MOR between

parallel and perpendicular directions (Fig. 4.2 *versus* Fig. 4.3 and Fig. 4.4 *versus* Fig. 4.5). Both un-waxed and waxed unidirectional specimens shown greater MOE/MOR along the parallel *versus* the perpendicular direction. For example, un-waxed specimens with parallel grain and an average density of 600 kg/m^3 tested in dry condition reached an average MOE value of 7162 MPa which is 10 times greater than that of similar specimens with perpendicular grain direction (723 MPa). This trend is also seen for flexural strength results (Figures 4.4 and 4.5). The MOR for the parallel un-waxed specimens with an average density of 600 kg/m^3 (tested dry) reached an average bending strength of 39 MPa *versus* 5.1 MPa their perpendicular counterparts (approx. 8 times difference). Similar trends were observed for all conditions tested. These results are not unexpected as the wood possesses higher strength and stiffness parallel than the perpendicular to the grain direction [105]. Moreover, the results are in agreement with the research of Chen et al [51], who investigated the effect of a panel density on mechanical properties of multidirectional OSB in both principal directions.

A clear relationship was also found between the bending properties and panel density for all unidirectional OSB specimens tested (Fig. 4.2 to 4.5). Strength and stiffness properties increased with an increase of panel density (in the range tested), indicating that the higher compaction ratio of the panel resulted in an improvement of the bending properties of OSB in the two principal directions. This can be explained by the fact that the higher densification promotes better contact between strands that resulted in improved bonding which enhances in-plane stiffness and strength. For example, un-waxed specimens at 0% MC (parallel grain) had MOE values increase from 5,636 to 8,004 MPa, and an increase in MOR from 30 to 50 MPa when the board density was increased from 480 to 657 kg/m^3. A similar result can be seen for perpendicular MOE

and MOR values. This result agrees with the most studies where an increase in panel density increases values for strength and stiffness [49, 51, 92, 106–108].

This increase in MOE and MOR with increasing density, however, is more prominent at lower MC levels (MC $\leq$ 25%) for all conditions tested. At higher MC levels (MC $\geq$ 50%), the effect of density becomes significantly less dominant as noted by the flattening slopes in Figures 4.2 to 4.5. For instance, waxed specimens at a MC of 10% (parallel grain) saw MOE values increase from 4,274 to 6,920 MPa (approx. 1.6 times increase) and the MOR values increased from 27.5 to 45.1 MPa (approx.1.6 times increase) when the board density increased from 525 to 666 kg/m^3. At a MC of 50%, the increase in MOE and MOR with increasing density was only 1.1 and 1.2 times, respectively when the board density increased from 515 to 644 kg/m^3.

Finally, the effect of wax content was found to have a relatively small effect on MOE and MOR as seen in Figures 4.2 to 4.5. While the addition of wax in OSB significantly affected the moisture kinetics (diffusivity) and total amount of moisture absorbed in the unidirectional panels (as shown in Chapter 3), the differences in mechanical properties (no wax *versus* wax) at specific average moisture contents was limited.

In order to assess the significance of the various parameters investigated, an ANOVA statistical analysis of the regression curves was performed to determine the impact of board density and wax content on the bending properties of the unidirectional OSB specimens (as a function of moisture content and grain orientation). The results of the statistical analysis are presented in Table 4.2 and 4.3 for MOE and MOR, respectively.

The resulting F-values and the probabilities (Pr(>|F|)) indicate a strong relationship (at a 5% significance level) between parallel or perpendicular MOE/MOR and board density at low MC levels (MC< 25%). As shown in the statistical analysis and by the experimental data, the board

density significantly affects the mechanical properties of OSB. Moreover, the statistical analysis at the 5% significance level reveals that the board density at MC levels > 25% was not a significant variable on the strength and stiffness in parallel and perpendicular MOR (Table 4.3) and parallel MOE (Table 4.2). In terms of wax content effects, the Pr(>|F|) values obtained for the ANOVA (Table 4.2 and 4.3) showed no significant effect in a majority of the cases, however, there were no consistent trends with respect to grain orientation or MC. The mixed results are also represented by other studies in the literature. Studies by Muehl et al [109], Iwakiri et al [110] and Mendes et al [111] concluded that the wax addition did not show a significant effect on tensile modulus MOE, however, findings from Lehmann [112], and Winistorfer et al [35] demonstrated that the mechanical properties of OSB deteriorate as wax addition increases above an effective limit of 2-3%.

Table 4.2 Results of the analysis of variance (F and P values) for linear fit of MOE as function of density board and wax content at different MC levels in parallel and perpendicular direction

Parallel specimens				Perpendicular specimens			
MC	**Factor**	**F Value**	**Pr(>|F|)**	**MC**	**Factor**	**F Value**	**Pr(>|F|)**
0%	Density	37.05	2.0×10^{-7}***	0%	Density	76.69	$8.\times 10^{-12}$***
	Wax	1.44	2.4×10^{-1} NS		Wax	0.74	3.9×10^{-1} NS
10%	Density	51.32	3.7×10^{-9}***	10%	Density	82.24	1.2×10^{-11}***
	Wax	13.812	5.2×10^{-4}***		Wax	0.23	6.4×10^{-1} NS
25%	Density	9.54	3.3×10^{-3}**	25%	Density	22.41	2.4×10^{-5}***
	Wax	3.98	5.2×10^{-2} NS		Wax	1.69	2.0×10^{-1} NS
50%	Density	0.28	6.0×10^{-1} NS	50%	Density	10.16	2.7×10^{-3}**
	Wax	17.32	1.4×10^{-4}***		Wax	20.46	4.7×10^{-5}***
80%	Density	0.004	9.5×10^{-1} NS	80%	Density	10.91	2.5×10^{-3}**
	Wax	0.44	5.1×10^{-1} NS		Wax	11.50	2.0×10^{-3}**

***: Significant at [0, 0.001] probability level
**: Significant at (0.001, 0.01] probability level
*: Significant at (0.01, 0.05] probability level
NS: Not significant at (0.05, 1] probability level

Table 4.3 Results of the analysis of variance (F and P values) for linear fit of MOR as function of density board and wax content at different MC levels in parallel and perpendicular direction

Parallel specimens				Perpendicular specimens			
MC	**Factor**	**F Value**	**Pr(>|F|)**	**MC**	**Factor**	**F Value**	**Pr(>|F|)**
0%	Density	72.36	4.5×10^{-11}***	0%	Density	33.55	4.1×10^{-7}***
	Wax	3.53	6.6×10^{-2} NS		Wax	11.50	1.3×10^{-3}**
10%	Density	35.70	2.6×10^{-7}***	10%	Density	33.49	6.9×10^{-7}***
	Wax	9.78	3.0×10^{-3}**		Wax	2.32	1.3×10^{-1} NS
25%	Density	16.46	1.8×10^{-4}***	25%	Density	18.00	1.4×10^{-4}***
	Wax	1.98	1.7×10^{-1} NS		Wax	0.11	7.4×10^{-1} NS
50%	Density	1.84	1.8×10^{-1} NS	50%	Density	0.99	3.2×10^{-1} NS
	Wax	0.04	8.4×10^{-1} NS		Wax	0.67	4.2×10^{-1} NS
80%	Density	2.93	9.9×10^{-2} NS	80%	Density	9.07	5.4×10^{-3}**
	Wax	6.97	1.4×10^{-2}*		Wax	0.16	6.8×10^{-1} NS

***: Significant at [0, 0.001] probability level
**: Significant at (0.001, 0.01] probability level
*: Significant at (0.01, 0.05] probability level
NS: Not significant at (0.05, 1] probability level

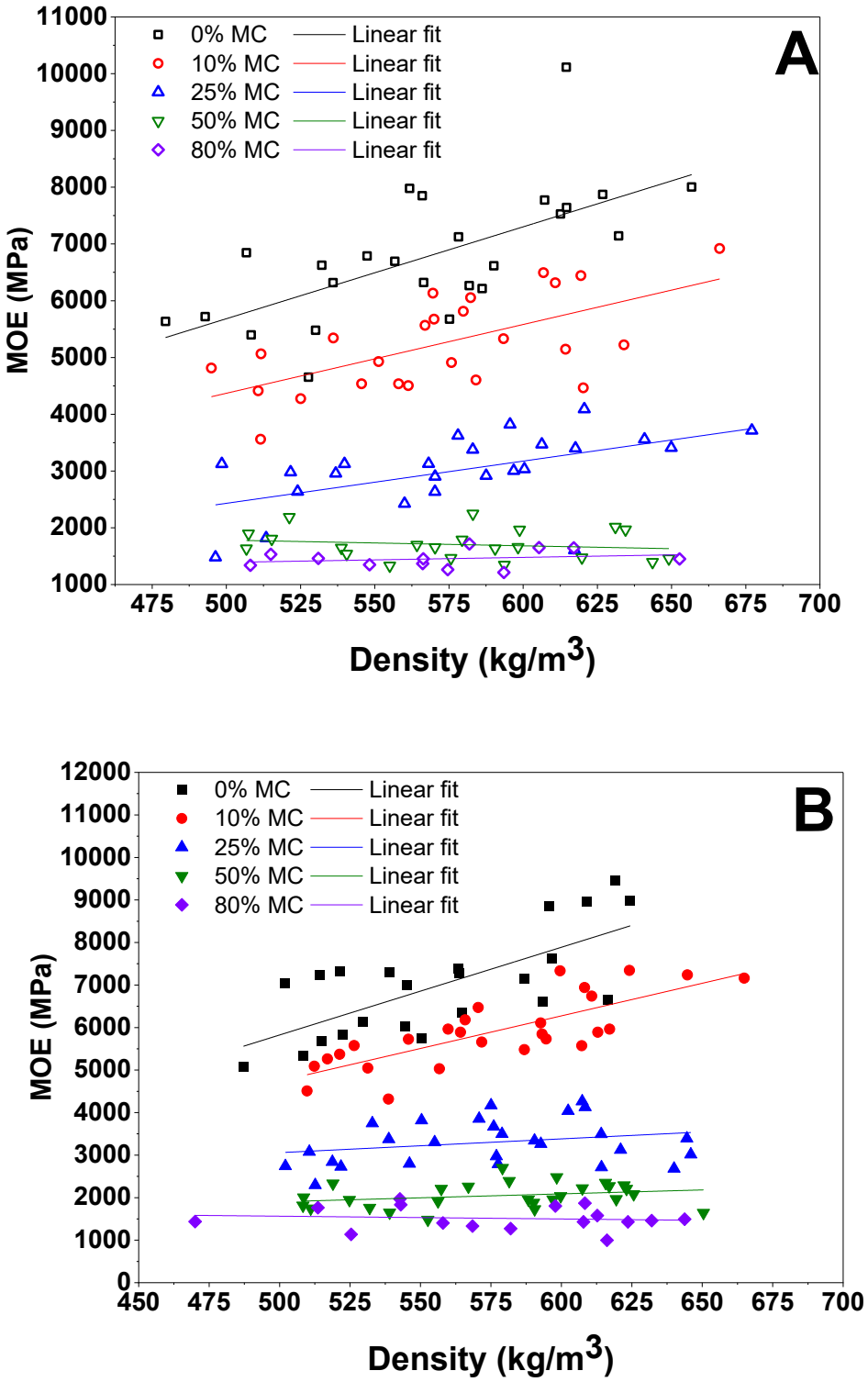

Figure 4.2 Bending parallel modulus of elasticity (MOE) of OSB as a function of density specimen for un-waxed (A) and waxed (B) samples

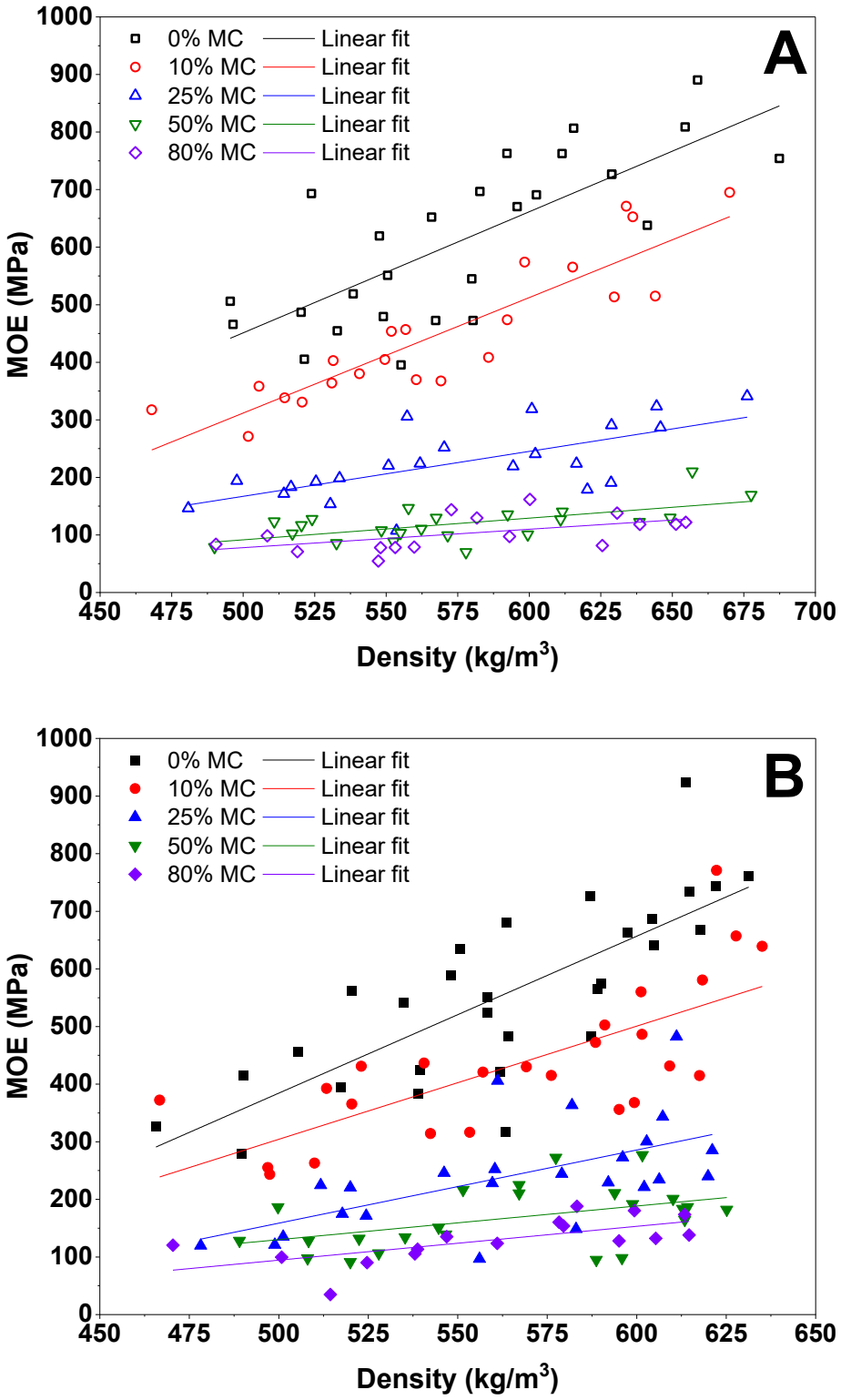

Figure 4.3 Bending perpendicular modulus of elasticity (MOE) of OSB specimens as a function of density for un-waxed (A) and waxed (B) specimens

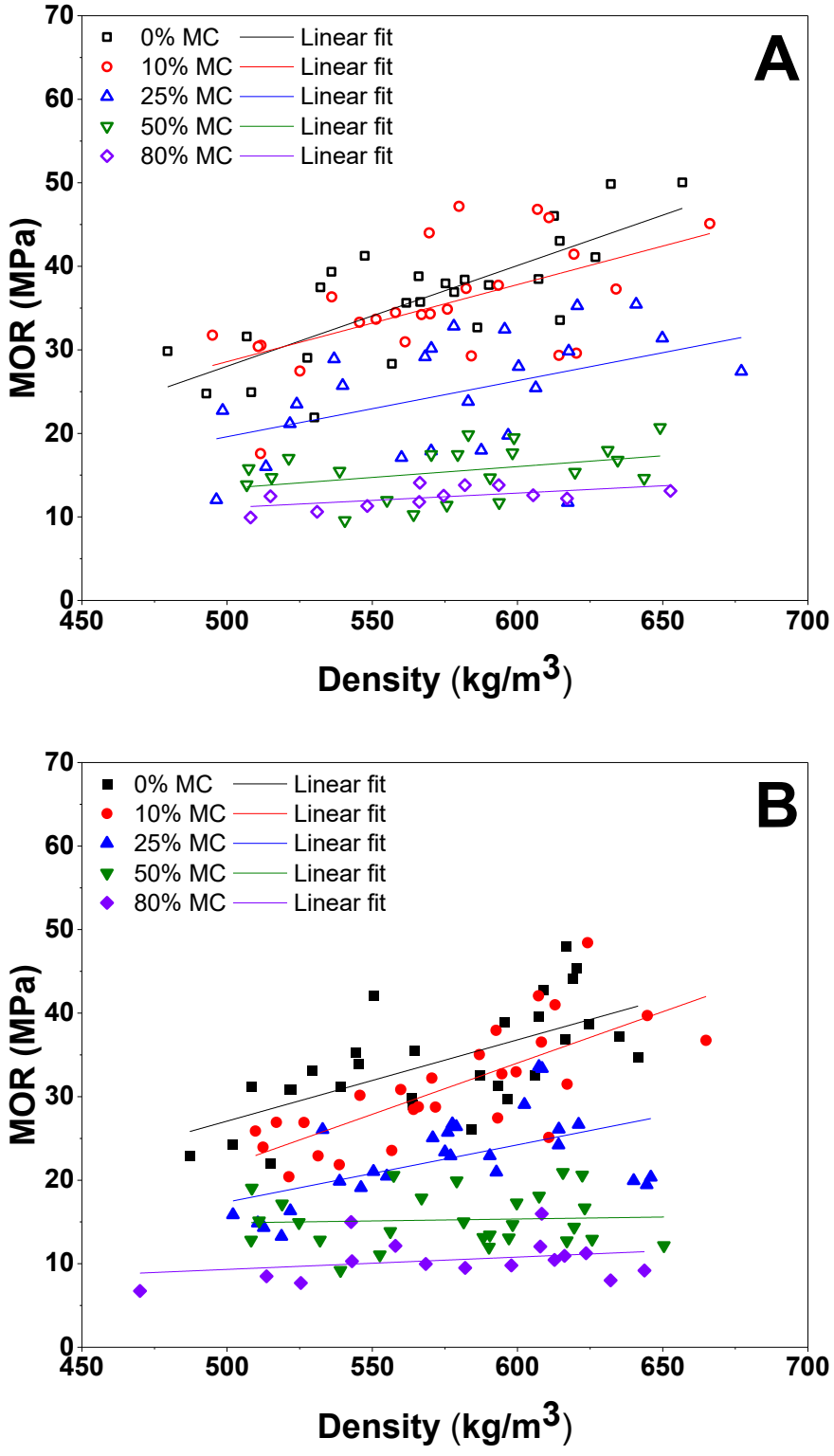

Figure 4.4 Bending parallel modulus of rupture (MOR) of OSB as a function of specimen density for un-waxed (A) and waxed (B) samples

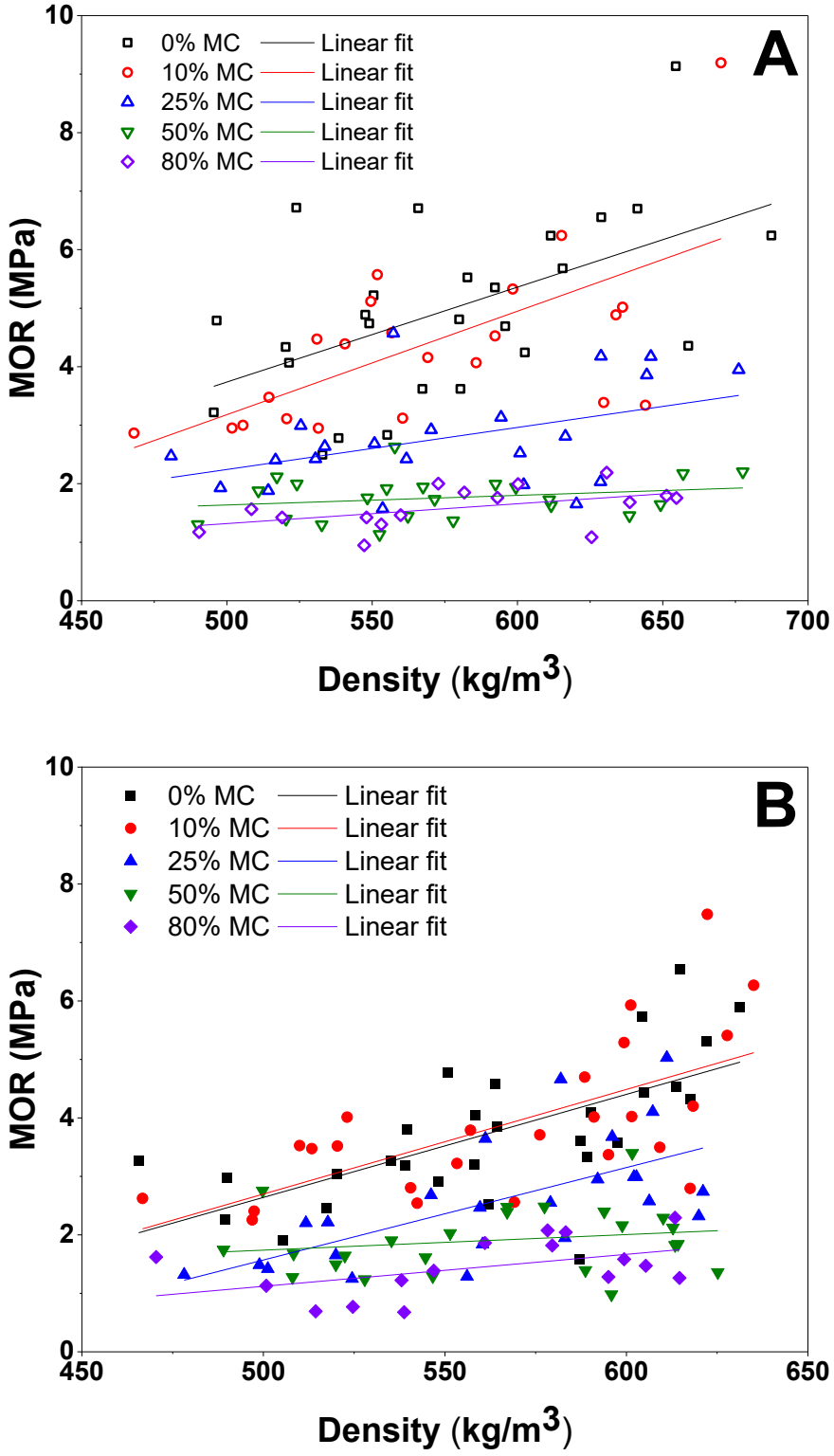

Figure 4.5 Bending perpendicular modulus of rupture (MOR) of OSB as a function of specimen density for un-waxed (A) and waxed (B) samples

4.3.3 Empirical model for unidirectional OSB panels

A set of empirical relationships for MOE and MOR was developed for the unidirectional panels tested in this study (in both parallel and perpendicular grain orientations) as a function of moisture content and panel density (with a relatively uniform VDP). These models were created as a potential tool for future modeling activities for OSB which require unidirectional mechanical properties as a function of the local density and MC. The data obtained in this study was fit and statistically analyzed using the curve-fitting toolbox in MATLAB R2019a. The *Bisquare* method was used to determine the regression parameters (p_{xy} and q_{xy}). It should be noted that wax content was excluded from this model since it's effect on MOE and MOR was found to be insignificant in a majority of test cases (see section 4.3.2).

First and second-order coefficients were tested to determine the best correlation between experimental and predicted MOE and MOR. The best correlation between the parallel and perpendicular bending properties was obtained considering a linear term for board density and quadratic term for MC (Eq. 4.4 and 4.5):

$$MOE(MC,\rho) = p_{00} + p_{10} * \rho + p_{01} * MC + p_{11} * MC * \rho + p_{02} * MC^2 \quad (4.4)$$

$$MOR(MC,\rho) = q_{00} + q_{10} * \rho + q_{01} * MC + q_{11} * MC * \rho + q_{02} * MC^2 \quad (4.5)$$

where MC is the moisture content, ρ is the panel density and p_{xy} and q_{xy} are the respective regression parameters. The regression parameters and correlation coefficient (R^2) for the relationships between MOE/MOR, density, and MC of OSB specimens are summarized in Table 4.4, and Figures 4.6 and 4.7.

As shown in the Figures 4.6 and 4.7, both density and MC have a significant effect on MOE and MOR. Furthermore, there is no appreciable difference observed between the MOE and MOR for un-waxed and waxed samples (red and blue dots). From Table 4.4, it can be seen that the statistical analysis showed a reasonable goodness of fit to the experimental data (Adj. R^2) for both the MOE and MOR regression models. The goodness of fit for the MOE model (0.9242 and 0.8773) was found to be better than that of the MOR model (0.7874 and 0.7270), and overall, both models had better fits to data from tests on samples with parallel orientations *versus* perpendicular.

Table 4.4 Regression results on the relationships between MOE/MOR, panel density, and MC for OSB specimens along parallel and perpendicular directions

	MOE	
Coefficients	**Parallel specimens**	**Perpendicular specimens**
p_{00}	-755	-587
p_{10}	13.52	2.04
p_{01}	-48.48	-0.27
p_{11}	-0.21	0.03
p_{02}	1.25	0.11
$Adj.R^2$	0.9242	0.8773
RMSE	615.1	73.28
	MOR	
Coefficients	**Parallel specimens**	**Perpendicular specimens**
q_{00}	23.16	2.601
q_{10}	2.972	0.46
q_{01}	-10.27	-1.28
q_{11}	-1.65	-0.24
q_{02}	2.07	0.37
$Adj.R^2$	0.7874	0.7270
RMSE	4.906	0.8362

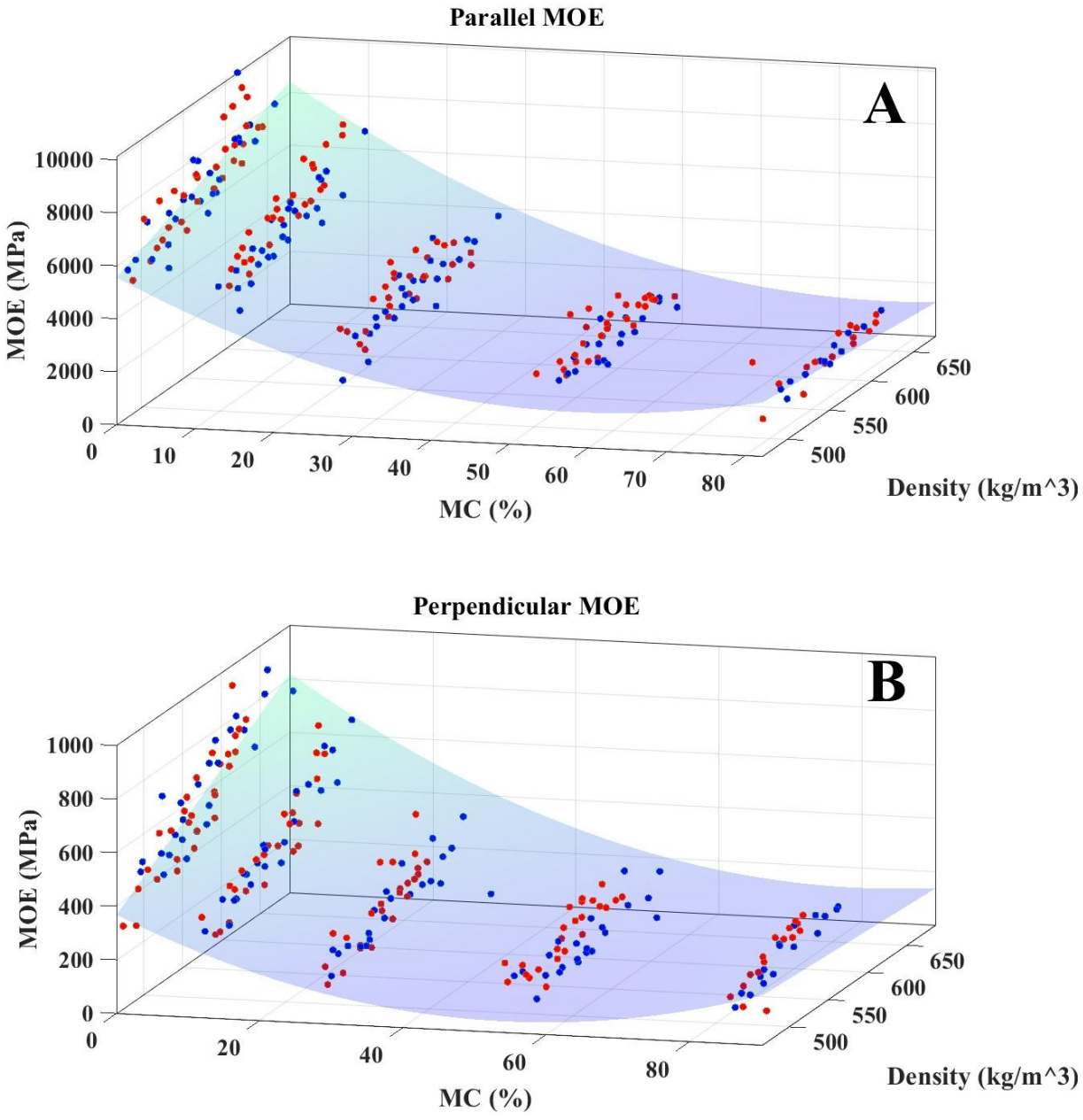

Figure 4.6 Modulus of Elasticity (MOE) of unidirectional specimens tested as a function of specimen density and average moisture content (MC) for (A) parallel and (B) perpendicular strand orientations. Blue and red dots represent un-waxed and waxed samples, respectively

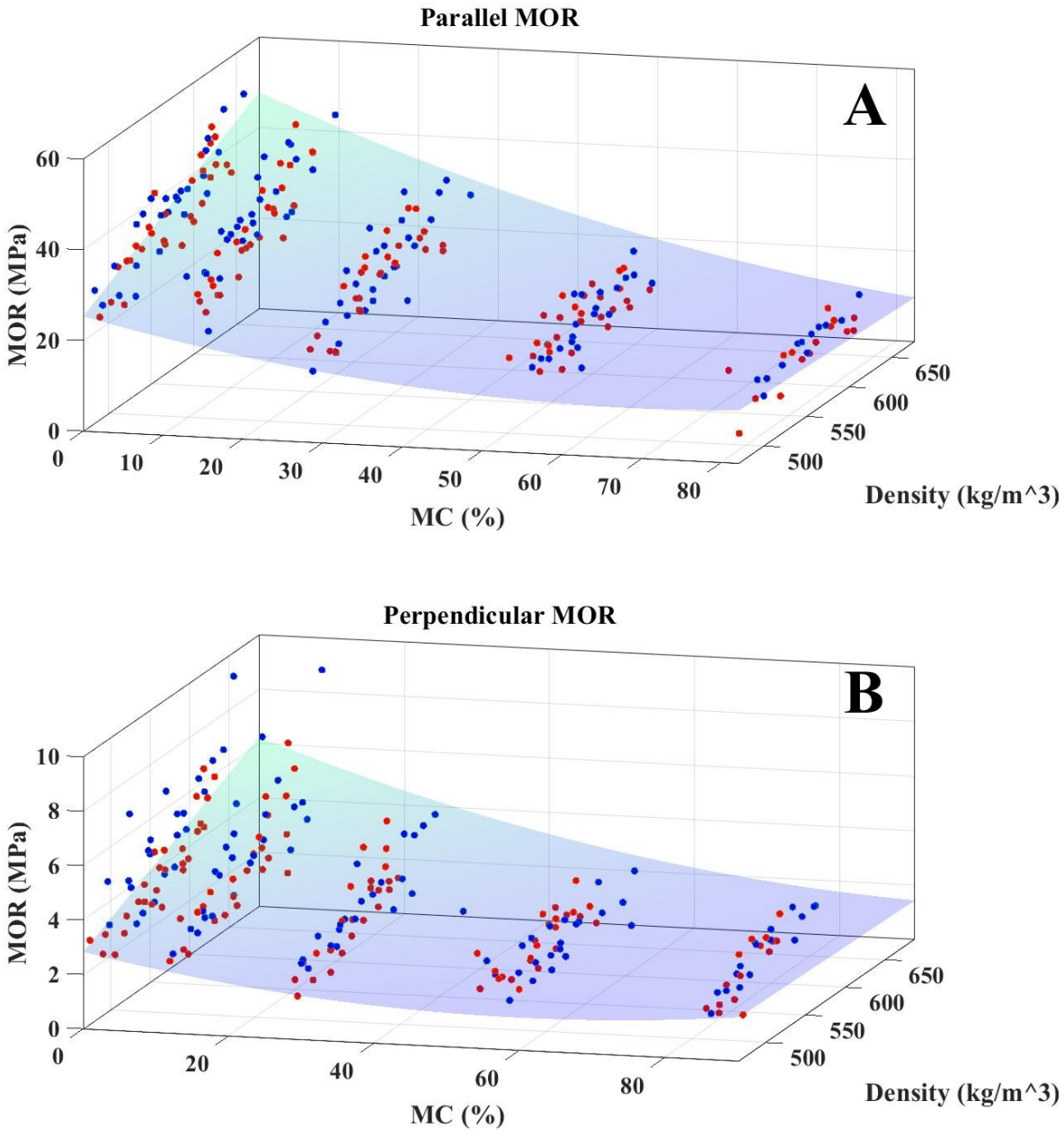

Figure 4.7 Modulus of Rupture (MOR) of unidirectional specimen tested as a function of specimen density and average moisture content (MC) for (A) parallel and (B) perpendicular strand orientations. Blue and red dots represent un-waxed and waxed samples, respectively

4.4 Conclusions

This study shows the relationship between thickness swell, bending strength and stiffness of unidirectional OSB as a function of moisture content, board density and wax content in both parallel and perpendicular directions. The result show that for unidirectional homogeneous panels, density is the most import parameter affecting thickness swell (TS) followed by moisture content (MC). Panel grain orientation was observed to have a significant effect on TS, but only at lower moisture contents (< 25%), while wax content was not found to be a significant factor in TS behavior.

In terms of mechanical properties, the results show that panel density, moisture content, and grain direction all had a significant effect on bending properties. Generally, modulus of elasticity (MOE) and modulus of rupture (MOR) both improved with increased panel density, and were both significantly higher for parallel *versus* perpendicular grain orientations. Moisture content was also seen to significantly affect both MOE and MOR. As MC increased, there was a noticeable decrease in both MOE and MOR for both parallel and perpendicular grain orientations. There was also an interaction effect between density and MC. For MC $\leq$ 25%, the bending properties improved rapidly with increasing panel density. However, for MC > 25%, the changes in bending properties with increasing density was not as significant. Wax content was also not found to have a significant effect on MOE and MOR for a majority of conditions tested.

Based on the experimental results, an empirical model was developed to predict MOE and MOR in unidirectional OSB panels as a function of board density, MC and grain direction. The relations are based on a polynomial equation with first order coefficients for panel density and second-order coefficients for MC. Separate MOE and MOR equations were developed for both parallel and perpendicular grain orientations, and all had reasonable fits to the experimental data.

Overall, this study on unidirectional OSB with a uniform vertical density profile provides a comprehensive and unique set of experimental data for future design and analysis of improved OSB panels subjected to moisture. The results and empirical model presented also provide key inputs and insights for the development of more advanced modeling approaches for OSB that require input properties at the ply (lamina) level.

Chapter 5: Conclusions and recommendations

5.1 Summary of key findings

In this thesis, the influence of panel density, grain direction and wax content on the diffusivity coefficient, thickness swell and mechanical properties of unidirectional OSB panels under different moisture conditions was studied and predicted in an effort to contribute to a better understanding of moisture transport effect on the service life and quality of oriented strand board or OSB (refer to Chapter 3). A finite element model based on Fick's second law was also developed to model the moisture transport in OSB, and was found to accurately fit the experimental data during the first stages of moisture absorption. It was found that moisture absorption behavior and the resulting diffusivity coefficients of OSB specimens were dependent on panel density, grain direction and wax content. The rate of moisture absorption (diffusivity coefficient) for waxed specimens markedly decreased compared to the un-waxed specimens which indicates that the wax slows down the initial absorption of moisture due to its hydrophobic nature (water repellency). In addition, the strands treated with wax helped to create better dimensional stability in the OSB panel over time due to the delay in water uptake within the panel. The diffusivity coefficient by the OSB specimens was strongly influenced by the grain direction with higher values along the parallel-to-grain direction compared to the perpendicular-to-grain direction. This was attributed to the natural cell (lumen) structure of the wood in the grain direction. With increasing density, the moisture absorption rate and water uptake decreased in both un-waxed and waxed specimens. This behavior was attributed to the increased compaction of the boards which promotes a higher strand-strand contact that may reduce the void spaces which contribute to water transport.

In terms of the effect of moisture content on thickness swell (TS) and bending properties, an extensive experimental design was used to investigate the effects of panel density (between 466-677 kg/m^3), wax content (0% and 2%) and grain orientation at different moisture levels (0, 10, 25, 50, and 80%). The results shown in Chapter 4 demonstrated that board density, grain directions, and moisture content have a significant influence on the response variables evaluated. Specifically, MOE and MOR improved as panel density increased, and decreased as average MC increased. Furthermore, density was found to be the most important parameter affecting TS with an increasing TS as density decreases. However, wax content did not have a significant effect on TS or bending properties in a majority of conditions tested. The relationship between board density and MC on parallel and perpendicular MOE and MOR was described by a polynomial mathematical model with first order coefficients for panel density and second-order coefficients for MC. These equations demonstrated a reasonable fit to the experimental data.

Based on the findings of this thesis research, the moisture diffusion model (Chapter 3) and the empirical relationship for bending properties of OSB (Chapter 4) show a potential to be used to the development of a Finite Element Model that takes into account the variation on MOE and MOR with the variations of local board density, moisture content, grain direction and wax content. In addition, the findings may provide a valuable contribution to the wood science community as potential input to more comprehensive models to predict to mechanical properties and thickness swell as a function of moisture ingress.

5.2 Novelty of work and recommendations for future work

The main objective of this thesis research was to investigate the effect of various OSB parameters such as panel density, grain directions and wax content on the moisture absorption and mechanical behaviour of OSB under different moisture conditions. Many researchers have studied the effect of moisture content on wood-based composites, however, very few studies have reported the relationship between the moisture content on the mechanical properties (including MOE and MOR). The unique aspect of this current work is that it entails the use of unidirectional OSB panels with a relatively uniform vertical density profile (VDP). The advantage of this approach is that primary properties (e.g., diffusivity, MOE) can be characterized for specific densities which can be used for the development of more advanced models. This is contrary to most studies which use conventional multidirectional OSB geometries with significant variation in density through the panel thickness (i.e. higher at the faces and lower in the core).

Furthermore, the comprehensive findings from this thesis research provides reliable results of various important parameters including the effect of panel density, grain orientation and wax content for both dry and wet OSB panels (at various MC levels). The results are also analyzed using advanced statistical methods to assess significance between these parameters. The base data and models developed (both empirical and finite element) can potentially be used by the wood science community to advance predictive modeling in OSB (especially in scenarios where moisture is an issue), and will also contribute to the existing research literature in this field.

Finally, there are a few recommendations for future extensions to this work:

- Investigating other wood species in terms of moisture absorption to better understand how this would affect their mechanical properties, and to build on data for a more expansive simulation tool to predict the effects of moisture exposure.

- A more comprehensive investigation on wax content and type on the performance of unidirectional OSB should also be considered. The goal will be to find the optimal value for various board applications while minimizing the cost of wax in the board.
- Investigate other types and amounts of resins and their mixtures such as those with different water resistance or hydrophobicity characteristics (e.g., MDI). These could be applied to the OSB manufacturing process to investigate if these resins are capable of generating boards with better water repellence and physical/mechanical properties.
- Investigate the effect of moisture absorption and diffusivity coefficient after exposure to different temperatures to improve the prediction of moisture transport under different ambient conditions.
- Develop a more comprehensive finite element (FE) model which can predict thickness swell and mechanical performance of dry and wet commercial OSB panels under both 3-point bending and/or concentrated static load (CSL) tests. This FE model would ultimately include the findings of this research, specifically the mechanical property relations of OSB as a function of board density, wax content, and moisture content.
- Finally, a more comprehensive experimental investigation into the moisture transport mechanisms in OSB at both the macro- and microscale. This would include further investigation and validation of X-ray tomography as a way to perform full-field mapping of moisture over time, and correlate these variations with measured (experimental) or predicted (model) properties.

Bibliography

1. Stark NM, Cai Z, Carll C (2010) Wood-based composite materials: Panel products, glued-laminated timber, structural composite lumber, and wood-nonwood composite materials. Wood Handb wood as an Eng Mater chapter 11 Centen ed Gen Tech Rep FPL; GTR-190 Madison, WI US Dept Agric For Serv For Prod Lab 2010 p 111-1128 190:11
2. APA (2017) Oriented Strand Board Product Guide. The Engineered Wood Association, https://www.apawood.org/publication-search?q=W410&tid=1. Accessed June 2021
3. FAO statistical database http://faostat. fao.org/, accessed August 2021
4. Cai Z, Ross RJ (2010) Mechanical properties of wood-based composite materials. Wood Handb wood as an Eng Mater chapter 12 Centen ed Gen Tech Rep FPL; GTR-190 Madison, WI US Dept Agric For Serv For Prod Lab 2010 p 121-1212 190:11–12
5. Howard JL, McKeever DB (2012) US forest products annual market review and prospects, 2008–2012. USDA For Serv For Prod Lab Res Note FPL-RN-0328, 2012 328:1–13
6. Kline DE (2007) Gate-to-gate life-cycle inventory of oriented strandboard production. Wood fiber Sci 37:74–84
7. Groom S (2005) Plywood vs. OSB. Fine Homebuilding 169 https://www.greenbuildingadvisor.com/app/uploads/sites/default/files/Plywood-vs-OSB_FHB169.pdf. Accessed June 2021
8. Wu Q, Piao C (1999) Thickness swelling and its relationship to internal bond strength loss of commercial oriented strandboard. For Prod J 49:50–55
9. Choi BY (2008) Using fungicides or combinations of fungicides to provide mold and decay fungal protection to OSB MSc thesis, Kookmin University, Seoul, South Korea
10. Barnes D (2001) A model of the effect of strand length and strand thickness on the strength properties of oriented wood composites. For Prod J 51:36
11. Chen S, Fang L, Liu X, Wellwood R (2008) Effect of mat structure on modulus of elasticity of oriented strandboard. Wood Sci Technol 42:197–210
12. Chen S, Du C, Wellwood R (2008) Analysis of strand characteristics and alignment of commercial OSB panels. For Prod J 58:94
13. Han G, Wu Q, Lu JZ (2007) Selected properties of wood strand and oriented strandboard from small-diameter southern pine trees. Wood fiber Sci 38:621–632
14. Fakhri HR, Semple KE, Smith GD (2007) Permeability of OSB. Part I. The effects of core fines content and mat density on transverse permeability. Wood fiber Sci 38:450–462
15. Fakhri HR, Semple KE, Smith GD (2007) Transverse permeability of OSB. Part II. Modeling the effects of density and core fines content. Wood fiber Sci 38:463–473
16. Han G, Wu Q, Lu JZ (2007) The influence of fines content and panel density on properties of mixed hardwood oriented strandboard. Wood Fiber Sci 39:2–15

17. Wang, Winistorfer PM (2000) Fundamentals of vertical density profile formation in wood composites. II. Methodology of vertical density formation under dynamic conditions. Wood fiber Sci J Soc Wood Sci Technol VO - 32 32:220–238

18. Hermawan A, Ohuchi T, Tashima R, Murase Y (2007) Manufacture of strand board made from construction scrap wood. Resour Conserv Recycl 50:415–426

19. Brochmann J, Edwardson C, Shmulsky R (2004) Influence of resin type and flake thickness on properties of OSB. For. Prod. J. 54:51–55

20. Kamke FA, Lee JN (2007) Adhesive penetration in wood - a review. Wood Fiber Sci. 39:205–220

21. Linville JD (2000) The influence of a horizontal density distribution on moisture-related mechanical degradation of oriented strand composites PHd thesis, Washinton State University, Washinton, United States of America

22. Barbuta C, Blanchet P, Cloutier A (2012) Mechanical properties of unidirectional strand board (USB) with flat vertical density profile. J Mater Sci Res 1:42

23. Kelly MW (1977) Critical literature review of relationships between processing parameters and physical properties of particleboard

24. Mackerle J (2005) Finite element analyses in wood research: a bibliography. Wood Sci. Technol. 39:579–600

25. Shmulsky R, Jones PD (2019) Forest products and wood science : an introduction., Seventh ed. John Wiley & Sons, Inc.

26. Spelter H (2006) Status and trends: Profile of structural panels in the United States and Canada. US Department of Agriculture, Forest Service, Forest Products Laboratory

27. Irle M, Barbu MC (2010) Wood-based panels: An introduction for specialists Thoemen M, Irle M and Sernek M (eds) Cost Action E49

28. Milner HR, Woodard AC (2016) Sustainability of engineered wood products. In: Sustainability of construction materials. Elsevier, pp 159–180

29. Moslemi AA (1974) Particleboard. Carbondale,USA, Southern Illinois University Press, 1974

30. Paridah MT, Ong LL, Zaidon A, et al (2006) Improving the dimensional stability of multi-layered strand board through resin impregnation. J Trop For Sci 166–172

31. Maloney TM (1977) Modern particleboard & dry-process fiberboard manufacturing. San Francisco, Calif. : Miller Freeman, c1977.

32. Wang K, Lam F (1997) Quadratic RSM models of processing parameters for three-layer oriented flakeboards. Wood fiber Sci 31:173–186

33. Wang, Lam F (1998) Computational modeling of material failure for parallel-aligned strand based wood composites. Comput Mater Sci 11:157–165

34. Meyers KL (2001) Impact of strand geometry and orientation on mechanical properties of strand composites MSc thesis, Washington State University, USA

35. Winistorfer PM, McFarland DL, Slover RC (1992) Evaluating the performance of ten wax formulations and three application rates on properties of oriented strand board. In: International Particleboard/Composite Materials Symposium, 26, Proceedings, Pullman, pp 236-250

36. Wang, Winistorfer PM, Young timothy M (2004) Fundamentals of Vertical Density Profile Formation in Wood Composites. Part III. MDF Density Formation During Hot-Pressing. Wood fiber Sci VO - 36 36:17–25

37. Carll C, Wiedenhoeft AC (2009) Moisture-related properties of wood and the effects of moisture on wood and wood products. Moisture Control Build key factor mold Prev 2nd ed West Conshohocken, PA ASTM Int 54–79

38. Barnes D (2002) A model of the effect of orienter design and operating variables on the mean angular deviation of oriented wood strands. For Prod J 52:63

39. Barnes D (2002) A model of the effect of strand angle and grain angle on the strength properties of oriented veneer and strand wood composites. For. Prod. J. 52:39–47

40. Nishimura T, Amin J, Ansell MP (2004) Image analysis and bending properties of model OSB panels as a function of strand distribution, shape and size. Wood Sci Technol 38:297–309. https://doi.org/10.1007/s00226-003-0219-z

41. Neimsuwan T (2004) Effect of resin and wax ratio on OSB properties, MSc thesis, University of Tennessee, Knoxville, USA.

42. Taylor A, Wang S, Freitag C, Morrell JJ (2008) Properties of'enhanced'OSB subfloor panels. For Prod J 58:

43. Zhang Y, Jin J, Wang S (2007) Effects of resin and wax on the water uptake behavior of wood strands. Wood Fiber Sci 39:271–278

44. Neimsuwan T, Wang S, Via B (2013) Effect of processing parameters, resin, and wax loading on water vapor sorption of wood strands

45. Kruse K, Dai C, Pielasch A (2000) An analysis of strand and horizontal density distributions in oriented strand board (OSB). Holz als Roh- und Werkst 58:270–277. https://doi.org/10.1007/s001070050424

46. Dai C, Steiner PR (1994) Spatial structure of wood composites in relation to processing and performance characteristics. 2. Modelling and simulation of a randomly-formed flake layer network. Wood Sci Technol VO - 28 28:135–146

47. Xu W, Suchsland O (1998) Modulus of elasticity of wood composite panels with a uniform vertical density profile: A model. Wood Fiber Sci 30:293–300

48. Xu W (1999) Influence of vertical density distribution on bending modulus of elasticity of wood composite panels: a theoretical consideration. Wood fiber Sci J Soc Wood Sci Technol VO - 31 31:277–282

49. Jin J, Dai C, Hsu WE, Yu C (2009) Properties of strand boards with uniform and conventional vertical density profiles. Wood Sci Technol 43:559

50. Bozo AM (2002) Spatial variation of wood composites. PHd thesis, Washiton State University, Washinton, Estados Unidos of America

51. Chen S, Du C, Wellwood R (2010) Effect of panel density on major properties of oriented strandboard. Wood Fiber Sci 42:177–184

52. van Houts JH, Wang S, Shi H, et al (2004) Moisture movement and thickness swelling in oriented strandboard, part 1. Analysis using nuclear magnetic resonance microimaging. WOOD Sci. Technol. 38:617–628

53. Wu Q, Suchsland O (1996) Linear expansion and its relationship to moisture content change for commercial oriented strandboards. For Prod J 46:79

54. Xu W, Winistorfer PM (1995) Layer thickness swell and layer internal bond of medium density fiberboard and oriented strandboard. For Prod J 45:67

55. Xu W, Winistorfer PM, Moschler WW (2007) A procedure to determine water absorption distribution in wood composite panels. Wood fiber Sci 28:286–294

56. Moya L, Tze WTY, Winandy JE (2009) The effect of cyclic relative humidity changes on moisture content and thickness swelling behavior of oriented strandboard. Wood fiber Sci. 41:447–460

57. Lee JN, Wu Q (2007) In-plane dimensional stability of three-layer oriented strandboard. Wood fiber Sci 34:77–95

58. Wu Q, Lee JN (2002) Thickness swelling of oriented strandboard under long-term cyclic humidity exposure condition. WOOD FIBER Sci. 34:125–139

59. Wu Q, Ren Y (2007) Characterization of sorption behavior of oriented strandboard under long-term cyclic humidity exposure condition. Wood fiber Sci 32:404–418

60. Mirski R, Derkowski A (2010) Bending strength of OSB subjected to boiling test. For Wood Technol No 71 Warsaw 2010 515

61. Mirski R, Dziurka D, Wieruszewski M (2015) Properties of OSB boards after a few cycles of aging tests. Wood Res 60:633–644

62. Pu JH, Tang RC, Hse C-Y (1994) Creep behavior of sweetgum OSB: effect of load level and relative humidity. For Prod Journal, Vol 44 45-50

63. Bach L, Zhao NW, Cheng JJR (1993) Surface coating can reduce creep of oriented strandboard. For Prod J 43:43

64. Vun RY, Beall FC (2004) Monitoring creep-rupture in oriented strandboard using acoustic emission: Effects of moisture content, Holzforschung, 58 (2004), pp. 387-399

65. Rice RW, Redfern I (2016) Heat capacity and its variation with moisture content for plywood and oriented strand board sheathing produced by North American Mills. For Prod J 66:413–418

66. Vololonirina O, Coutand M, Perrin B (2014) Characterization of hygrothermal properties of wood-based products–Impact of moisture content and temperature. Constr Build Mater 63:223–233

67. Liping C, Deku S (1992) Modelling of the moisture transfer process in particleboards. Holz als Roh- und Werkst 50:395–399. https://doi.org/10.1007/BF02627609

68. Siau JF (1984) Transport processes in wood. Berlin Heidelberg New York: Springer-Verlag. p 131

69. Tackie alan D, Wang S, Bennett RM, Shi SQ (2008) Investigation of OSB thickness-swell based on a 3D density distribution. Part I. The finite element model. Wood fiber Sci J Soc Wood Sci Technol VO - 40 40:91–102

70. Cloutier A (2001) Finite element modeling of dimensional stability in layered wood composite. In: 35th international particleboard/composite materials symposium, 2001. Washington State University, pp 63–72

71. Tackie alan D, Wang S, Bennett RM (2008) Investigation of OSB thickness-swell based on a 3-D density distribution. Part II. Variations in thickness-swell and internal stresses. Wood fiber Sci J Soc Wood Sci Technol VO - 40 40:352–361

72. Chen Z, Yan N, Cooper P sh. HOLZ ALS ROH-UND Werkst. 66:207–212

73. Suzuki S, Miyamoto K (1998) Effect of manufacturing parameters on the linear expansion and density profile of particleboard. J wood Sci 44:444–450

74. Shen C-H, Springer GS (1976) Moisture absorption and desorption of composite materials. J Compos Mater 10:2–20

75. van Houts JH, Wang S, Shi H, Kabalka G (2006) Moisture movement and thickness swelling in oriented strandboard. Part 2: Analysis using a nuclear magnetic resonance imaging body scanner. WOOD Sci. Technol. 40:437–443

76. Hartley ID, Wang S, Zhang Y (2007) Water vapor sorption isotherm modeling of commercial oriented strand panel based on species groups and resin type. Build Environ 42:3655–3659

77. Gereke T, Hass P, Niemz P (2010) Moisture-induced stresses and distortions in spruce cross-laminates and composite laminates. Holzforschung 64:127–133. https://doi.org/10.1515/HF.2010.003

78. Wu Q, Suchsland O (1996) Prediction of moisture content and moisture gradient of an overlaid particleboard. Wood fiber Sci 28:227–239

79. Ganev S, Cloutier A, Gendron G, Beauregard R (2005) Finite element modeling of the hygroscopic warping of medium density fiberboard. WOOD FIBER Sci. 37:337–354

80. Shi S (2007) Diffusion model based on Fick's second law for the moisture absorption process in wood fiber-based composites: is it suitable or not. Wood Sci Technol 41:645–658. https://doi.org/10.1007/s00226-006-0123-4

81. Liping C, Wang F (1994) Steady and unsteady state moisture movement in particleboards. Holz als Roh- und Werkst 52:304–306. https://doi.org/10.1007/BF02621419

82. Thomen H (2000) Modeling the physical processes in natural fiber composites during batch and continuous pressing. Ph.D. Thesis, Oregon State University, USA

83. Pierron F, Poirette Y, Vautrin A (2002) A novel procedure for identification of 3D moisture diffusion parameters on thick composites: theory, validation and experimental results. J Compos Mater 36:2219–2243

84. Saidane EH, Scida D, Assarar M, Ayad R (2016) Assessment of 3D moisture diffusion parameters on flax/epoxy composites. Compos Part A Appl Sci Manuf 80:53–60

85. Brodowsky H, Mäder E (2007) Jute fibre/polypropylene composites II. Thermal, hydrothermal and dynamic mechanical behaviour. Compos Sci Technol 67:2707–2714

86. Cherif ZE, Poilâne C, Falher T, et al (2013) Influence of textile treatment on mechanical and sorption properties of flax/epoxy composites. Polym Compos 34:1761–1773

87. Cherif ZE, Poilâne C, Vivet A, et al (2016) About optimal architecture of plant fibre textile composite for mechanical and sorption properties. Compos Struct 140:240–251

88. Biblis EJ, Grigoriou A, Carino H (1996) Flexural properties of veneer-overlaid OSB composite panels from southern yellow pine. For Prod J 46:59

89. Papadopoulos AN (2006) A New Environmental Friendly Technology for the Production of Decay Resistant and Dimensional Stable Strandboard (OSB). Manag Dev Mt Isl Areas 20

90. Papadopoulos AN, Traboulay E (2002) Dimensional stability of OSB made from acetylated fir strands. Holz als Roh-und Werkst 60:84–87

91. APA (2018) PS 2-18 Performance Standard for Wood Structural Panels. The Engineered Wood Association, https://apawood-europe.org/wp-content/uploads/2020/01/S350.pdf

92. van Houts JH, Winistorfer PM, Wang S (2003) Analysis of OSB mat stucture made from industrially manufactured strands using simulation modeling. WOOD FIBER Sci. 35:351–362

93. Chang W (1999) Thickness swelling behaviour of oriented strand board MSc Thesis, University of Toronto, Canada

94. Dai C, Yu C, Zhou C (2007) Theoretical modeling of bonding characteristics and performance of wood composites. I. Inter-element contact. Wood fiber Sci J Soc Wood Sci Technol VO - 39 39:48–55

95. Xu W, Winistorfer PM (2007) A procedure to determine thickness swell distribution in wood composite panels. Wood fiber Sci 27:119–125

96. Olek W, Perré P, Weres J (2005) Inverse analysis of the transient bound water diffusion in wood. 59:38–45. https://doi.org/doi:10.1515/HF.2005.007

97. Crank J (1979) The mathematics of diffusion. Oxford university, Clarendon press

98. Zhu EC, Guan ZW, Pope DJ, Rodd PD (2007) Effect of Openings on Oriented Strand Board Webbed Wood I-Joists. J Struct Eng 133:145–149

99. Li W, Van den Bulcke J, De Windt I, et al (2013) Combining electrical resistance and 3-D X-ray computed tomography for moisture distribution measurements in wood products exposed in dynamic moisture conditions. Build Environ 67:250–259. https://doi.org/https://doi.org/10.1016/j.buildenv.2013.05.026

100. Wang S, Winistorfer PM (2003) An optical technique for determination of layer thickness swell of MDF and OSB. For Prod J 53:

101. Geimer RL (1982) Dimensional stability of flakeboards as affected by board specific gravity and flake alignment. For Prod journal Vol 32, no 8 (Aug 1982) Pages 44-52

102. Shmulsky R, Jones PD, Lilley K (2011) Forest products and wood science : an introduction., 6th ed. Wiley-Blackwell

103. Wu Q, Suchsland O (1997) Effect of moisture on the flexural properties of commercial oriented strandboards. Wood fiber Sci 29:47–57

104. Böhm M (2009) The influence of moisture content on thickness swelling and modulus of elasticity in oriented strand board bending. Wood Res 54:79–90

105. Desch HE, Dinwoodie JM (1981) Timber: its structure, properties and utilisation. MacMillan Press Ltd.

106. Turner HD (1954) Effect of particle size and shape on strength and dimensional stability of resin-bonded wood-particle panels. Prod J 4:210–223

107. Lynam TM, Hall WJ (1959) Studies of the strain distribution in wide plates during brittlefracture propagation Ship, Structures Committee Report Serial No. SSC-118, Washington: National Academy of Sciences, National Research Council

108. Stewart HA, Lehmann WF (1973) High-quality particleboard from cross-grain, knife-planed hardwood flakes. For Prod J

109. Muehl JH, Krzysik AM (1997) Ujtecaj smole i voska na mehanic'ka i fizikalna svojstva tvrdih vlaknatica proizvedenih suhim postupkom. Drv Ind 48:3–9

110. Iwakiri S, Mendes LM, Saldanha LK (2003) Production of Oriented Strand Board (OSB) from Eucalyptus Grandis with different resin content, wax sizing and face to core layer ratios. CiÆncia Florest

111. Farinassi Mendes R, Bortoletto Júnior G, Ferreira de Almeida N, et al (2013) Effects of thermal pre-treatment and variables of production on properties of OSB panels of Pinus taeda. Maderas Cienc y Tecnol 15:141–152

112. Lehmann WF (1978) Cyclic moisture conditions and their effect on strength and stability of structural flakeboards, Proc WSU Symp Particleboard 11:351–368